UNIVERSIDAD DE CONCEPCIÓN

Centro de Investigación en Ingeniería Matemática (CI^{2}MA)

Centro de Investigación en Ingeniería Matemática

An a posteriori error estimate for a dual mixed method applied to Stokes system with non null source terms

Tomás Barrios, Edwin Behrens,
Rommel Bustinza

PREPRINT 2020-27

SERIE DE PRE-PUBLICACIONES

An a posteriori error estimate for a dual mixed method applied to Stokes system with non null source terms

Tomás P. Barrios [*], Edwin M. Behrens [†] and Rommel Bustinza [‡]

Abstract

In this manuscript, we focus our attention in the Stokes flow with non homogeneous source terms, formulated in dual mixed form. For the sake of completeness, we begin recalling the corresponding well-posedness at continuous and discrete levels. After that, and with the help of a quasi Helmholtz decomposition technique, we develop a residual type a posteriori error analysis, deducing an estimator that is reliable and locally efficient. Finally, we provide numerical experiments, which confirm our theoretical results on the a posteriori error estimator and illustrate the performance of the corresponding adaptive algorithm, supporting its use in practice.

Mathematics Subject Classifications (1991): 65N15, 65N30, 65N50

Key words: A posteriori error estimates, dual mixed formulation, Stokes system.

1 Introduction

Dual mixed methods applied to Stokes system have been studied in [14], where the second order equation is rewritten as a first order system by introducing the flux as a new unknown. Then, the scheme is available to approximate simultaneously the flux, the velocity and the pressure. Existence and uniqueness is established using an appropriated norm, such that the discrete scheme admits the use of conforming Raviart-Thomas elements as finite element for the flux, and piecewise constants for the velocity and the pressure. The corresponding a posteriori error estimator has been developed in [15]. Alternatively, another dual mixed approach for the incompressible fluid flow has been introduced and analysed in [10]. The approach there follows the ideas developed in [9], i.e. the incompressible fluid flow is reformulated introducing the so-called pseudostress as an additional unknown, which is in relation with the pressure and gradient of the velocity. This allows us to eliminate the pressure, deriving a mixed variational formulation based on the pseudostress and the velocity. We remark

[*]Departamento de Matemática y Física Aplicadas, Universidad Católica de la Santísima Concepción, Concepción (Chile). E-mail: tomas@ucsc.cl

[†]Departamento de Ingeniería Civil, Universidad Católica de la Santísima Concepción, Concepción (Chile). E-mail: ebehrens@ucsc.cl

[‡]Centro de Investigación en Ingeniería Matemática (CI^2MA) & Departamento de Ingeniería Matemática, Universidad de Concepción, Casilla 160-C, Concepción (Chile). E-mail: rbustinz@ing-mat.udec.cl.

that the pseudostress is nonsymmetric and the approximation of the pressure, the velocity gradient (and thus the vorticity), or even the stress can be algebraically obtained from the approximate value of the pseudostress. The discrete scheme allows the use of the pair of conforming Raviart-Thomas and discontinuous piecewise polynomial as the finite element space. The a posteriori error analysis of the mixed pseudostress-velocity formulation of the Stokes problem has been established in [11]. Furthermore, in order to obtain more flexibility in the choice of finite element spaces, the stabilisation of this approach has been studied in [16] (also see [17]), and additionally its corresponding extension to quasi Newtonian flows and Brinkman model have been developed in [18] and [7], respectively.

Recently, in [3] we propose a stabilised mixed method to the Stokes system with nonhomogeneous source terms. There, we first introduced a dual mixed formulation, and then establishing the corresponding well-posedness at continuous and discrete levels, invoking the well-known Babuška-Brezzi theory. Then, our interest in this article is to endow this approach with an a posteriori error estimator. To this aim, and strongly motivated by the reduction of computational cost obtained with the a posteriori error estimator based on Ritz projection of the error, we endow the new approach with an a posteriori error analysis, following the ideas described in the previous work [5]. As a result, we deduce a nonstandard residual type a posteriori error estimator consisting of five terms for elements of the triangulation without edges on $\partial\Omega$, and seven terms for elements having an edge on $\partial\Omega$.

The rest of the paper is organised as follows. In Section 2, we recall the dual mixed variational formulation, the Galerkin scheme and the stable pairs of finite element subspaces. Section 3 is concerned with the a posteriori error analysis. Finally, in Section 4 we provide several numerical experiments that support the use of our a posteriori error estimator in practice.

We end this section with some notations to be used throughout the paper. Given a Hilbert space M, we denote by M^2 and $M^{2\times2}$ the space of vectors and square tensors of order 2 with entries in M, respectively. Given $\boldsymbol{\tau} := (\tau_{ij})$ and $\boldsymbol{\zeta} := (\zeta_{ij}) \in \mathbb{R}^{2\times2}$, we denote $\boldsymbol{\tau}^{\mathtt{t}} := (\tau_{ji})$, $\operatorname{tr}(\boldsymbol{\tau}) := \tau_{11} + \tau_{22}$ and $\boldsymbol{\tau} : \boldsymbol{\zeta} := \sum_{i,j=1}^{2} \tau_{ij}\,\zeta_{ij}$. Moreover, we introduce the deviator of $\boldsymbol{\tau}$ by $\boldsymbol{\tau}^{\mathtt{d}} := \boldsymbol{\tau} - \frac{1}{2}\operatorname{tr}(\boldsymbol{\tau})\boldsymbol{I}$, where $\boldsymbol{I} \in \mathbb{R}^{2\times2}$ denotes de identity tensor. In addition, given $\boldsymbol{v} := (v_i)\,,\ \boldsymbol{w} := (w_i) \in \mathbb{R}^2$, we define $\boldsymbol{v} \otimes \boldsymbol{w} := \big(v_i\,w_j\big) \in \mathbb{R}^{2\times2}$. We also use the standard notations for Sobolev spaces and norms. Finally, C or c (with or without subscripts) denote generic constants, independent of the discretization parameters, that may take different values at different occurrences.

2 The model problem and its dual mixed formulation

Let Ω be a bounded and simply connected domain in $\mathbb{R}^2$ with polygonal boundary Γ. Then, given the source terms $\tilde{f} \in L_0^2(\Omega) := \{q \in L^2(\Omega) : \int_\Omega q = 0\}$, $\boldsymbol{f} \in [L^2(\Omega)]^2$ and $\boldsymbol{g} \in [H^{1/2}(\Gamma)]^2$, we look for the velocity (vector field) $\boldsymbol{u}$ and the pressure (scalar field) p such that

$$-\nu\Delta\boldsymbol{u} + \nabla p = \boldsymbol{f} \quad \text{in} \quad \Omega\,, \qquad \operatorname{div}(\boldsymbol{u}) = \tilde{f} \quad \text{in} \quad \Omega\,, \quad \text{and} \quad \boldsymbol{u} = \boldsymbol{g} \quad \text{on} \quad \Gamma\,, \tag{1}$$

where $\nu > 0$ is the fluid viscosity of the flow and the datum data $\tilde{f}$ and $\boldsymbol{g}$ satisfies the compatibility condition $\int_\Gamma \boldsymbol{g}\cdot\boldsymbol{n} = 0$, with $\boldsymbol{n}$ being the unit outward normal at Γ. In addition, for uniqueness purposes, we seek $p \in L_0^2(\Omega)$.

Hereafter $\mathbf{div}$ stands for the usual divergence operator div acting along each row of the tensor. Our purpose is to apply dual mixed method. To this aim, we first reformulate problem (1) introducing the pseudostress $\boldsymbol{\sigma} := \nu\nabla\boldsymbol{u} - p\boldsymbol{I}$ in Ω as an additional unknown. Considering the condition $\mathrm{div}(\boldsymbol{u}) = \tilde{f}$ in Ω, we deduce that $p = \frac{\nu}{2}\tilde{f} - \frac{1}{2}\mathrm{tr}(\boldsymbol{\sigma})$ in Ω, and then $\boldsymbol{\sigma}$ belongs to $H_0 := \{\boldsymbol{\tau} \in H(\mathbf{div};\Omega) : \int_\Omega \mathrm{tr}(\boldsymbol{\tau}) = 0\}$. As a result, the pressure p can be eliminated from (1), which can be rewritten as the first order system: *Find* $(\boldsymbol{\sigma}, \boldsymbol{u}) \in H_0 \times [H^1(\Omega)]^2$ *such that*

$$\frac{1}{\nu}\boldsymbol{\sigma}^{\mathrm{d}} - \nabla\boldsymbol{u} = -\frac{1}{2}\tilde{f}\boldsymbol{I} \quad \text{in} \quad \Omega\,, \quad \mathbf{div}(\boldsymbol{\sigma}) = -\boldsymbol{f} \quad \text{in} \quad \Omega, \quad \text{and} \quad \boldsymbol{u} = \boldsymbol{g} \quad \text{on} \quad \Gamma\,. \tag{2}$$

We point out that in [3] we have deduced the mixed variational formulation associated to (2), which reads as: *Find* $(\boldsymbol{\sigma}, \boldsymbol{u}) \in H_0 \times [L^2(\Omega)]^2$ *such that*

$$\begin{aligned} a(\boldsymbol{\sigma}, \boldsymbol{\tau}) + b(\boldsymbol{\tau}, \boldsymbol{u}) = \quad & G(\boldsymbol{\tau}) \quad \forall\, \boldsymbol{\tau} \in H_0\,, \\ b(\boldsymbol{\sigma}, \boldsymbol{v}) = \quad & F(\boldsymbol{v}) \quad \forall\, \boldsymbol{v} \in [L^2(\Omega)]^2\,, \end{aligned} \tag{3}$$

where the bilinear forms $a : H(\mathbf{div},\Omega) \times H(\mathbf{div},\Omega) \to \mathbb{R}$ and $b : H(\mathbf{div},\Omega) \times [L^2(\Omega)]^2 \to \mathbb{R}$ are defined by

$$\begin{aligned} a(\boldsymbol{\rho}, \boldsymbol{\tau}) &:= \frac{1}{\nu}\int_\Omega \boldsymbol{\rho}^{\mathrm{d}} : \boldsymbol{\tau}^{\mathrm{d}} \quad \forall\, \boldsymbol{\rho}, \boldsymbol{\tau} \in H(\mathbf{div},\Omega)\,, \\ b(\boldsymbol{\tau}, \boldsymbol{v}) &:= \int_\Omega \boldsymbol{v}\cdot\mathbf{div}(\boldsymbol{\tau}) \quad \forall\,(\boldsymbol{\tau}, \boldsymbol{v}) \in H(\mathbf{div},\Omega) \times [L^2(\Omega)]^2\,. \end{aligned}$$

In addition, the linear functionals $G : H(\mathbf{div},\Omega) \to \mathbb{R}$ and $F : [L^2(\Omega)]^2 \to \mathbb{R}$ are given by

$$G(\boldsymbol{\tau}) := \langle \boldsymbol{\tau}\,\boldsymbol{n}, \boldsymbol{g}\rangle - \frac{1}{2}\int_\Omega \tilde{f}\,\mathrm{tr}(\boldsymbol{\tau}) \quad \forall\,\boldsymbol{\tau} \in H(\mathbf{div},\Omega) \quad \text{and} \quad F(\boldsymbol{v}) := -\int_\Omega \boldsymbol{f}\cdot\boldsymbol{v} \quad \forall\,\boldsymbol{v} \in [L^2(\Omega)]^2\,,$$

with $\langle\cdot,\cdot\rangle$ denoting the duality paring between $[H^{-1/2}(\Gamma)]^2$ and $[H^{1/2}(\Gamma)]^2$ with respect to $L^2(\Gamma)$-inner product. We provide $H(\mathbf{div},\Omega)$ and $[L^2(\Omega)]^2$ with their usual inner products and induced norms $||\cdot||_{H(\mathbf{div};\Omega)}$ and $||\cdot||_{[L^2(\Omega)]^2}$, respectively. Then, we define the product spaces $\boldsymbol{\Sigma} := H(\mathbf{div},\Omega) \times [L^2(\Omega)]^2$ and $\boldsymbol{\Sigma}_0 := H_0 \times [L^2(\Omega)]^2 \subseteq \boldsymbol{\Sigma}$, endowed with its standard norm

$$||(\boldsymbol{\tau}, \boldsymbol{v})||_{\boldsymbol{\Sigma}} := \left(||\boldsymbol{\tau}||^2_{H(\mathbf{div};\Omega)} + ||\boldsymbol{v}||^2_{[L^2(\Omega)]^2}\right)^{1/2} \quad \forall\,(\boldsymbol{\tau}, \boldsymbol{v}) \in \boldsymbol{\Sigma}\,.$$

We remark that the well-posedness of (3) is a consequence of Babuška-Brezzi's theory (cf. Theorem 1 in [3]). We point out that the important details can be seen in the proof of Theorem 2.3 in [10].

Now, in order to discuss the discretization of (3) with finite element technique, we consider that Ω is a polygonal region and let $\{\mathcal{T}_h\}_{h>0}$ be a shape-regular family of triangulations of $\bar{\Omega}$ such that $\overline{\Omega} = \cup_{T\in\mathcal{T}_h} T$. For each triangle $T \in \mathcal{T}_h$, h_T will denote its diameter, while the mesh size ot the triangulation is given by $h := \max\{\, h_T : T \in \mathcal{T}_h \,\}$. Moreover, given an integer $\ell \geq 0$ and a subset S of $\mathbb{R}^2$, we denote by $\mathcal{P}_\ell(S)$ the space of polynomials in two variables defined in S of total degree at most ℓ, and for each $T \in \mathcal{T}_h$, we define the local Raviart-Thomas space of order κ (cf. [22]),

$\mathcal{RT}_\kappa(T) := [\mathcal{P}_\kappa(T)]^2 \oplus \mathcal{P}_\kappa(T)\,\boldsymbol{x} \subseteq [\mathcal{P}_{\kappa+1}(T)]^2 \quad \forall \boldsymbol{x} \in T$. Then, for $k \in \mathbb{Z}_0^+$, we introduce the finite element subspaces

$$H_h^{\boldsymbol{\sigma}} := \left\{ \boldsymbol{\tau}_h \in H(\mathbf{div};\Omega) : \boldsymbol{\tau}_h|_T \in [\mathcal{RT}_k(T)^{\mathrm{t}}]^2, \quad \forall T \in \mathcal{T}_h \right\},$$

$$H_{0,h}^{\boldsymbol{\sigma}} := \left\{ \boldsymbol{\tau}_h \in H_h^{\boldsymbol{\sigma}} : \int_\Omega \mathrm{tr}(\boldsymbol{\tau}_h) = 0 \right\},$$

$$H_h^{\boldsymbol{u}} := \left\{ \boldsymbol{v}_h \in [L(\Omega)]^2 : \boldsymbol{v}_h|_T \in [\mathcal{P}_k(T)]^2, \quad \forall T \in \mathcal{T}_h \right\},$$

Now, setting $\boldsymbol{\Sigma}_{0,h} := H_{0,h}^{\boldsymbol{\sigma}} \times H_h^{\boldsymbol{u}}$, the corresponding discrete variational formulation of (3) reads as follows: *Find* $(\boldsymbol{\sigma}_h, \boldsymbol{u}_h) \in \boldsymbol{\Sigma}_{0,h}$ *such that*

$$\begin{aligned} a(\boldsymbol{\sigma}_h, \boldsymbol{\tau}) + b(\boldsymbol{\tau}, \boldsymbol{u}_h) &= G(\boldsymbol{\tau}) \quad \forall\, \boldsymbol{\tau} \in H_{0,h}^{\boldsymbol{\sigma}}, \\ b(\boldsymbol{\sigma}_h, \boldsymbol{v}) &= F(\boldsymbol{v}) \quad \forall\, \boldsymbol{v} \in H_h^{\boldsymbol{u}}, \end{aligned} \tag{4}$$

Applying a discrete version of Babuška-Brezzi's theory, we can establish that (4) has one and only one solution $(\boldsymbol{\sigma}_h, \boldsymbol{u}_h) \in \boldsymbol{\Sigma}_{0,h}$. Moreover, there exists $C > 0$, independent of h, such that

$$||(\boldsymbol{\sigma}_h, \boldsymbol{u}_h)||_{\boldsymbol{\Sigma}} \leq C \left(||\boldsymbol{f}||_{[L^2(\Omega)]^2} + ||\tilde{f}||_{L^2(\Omega)} + ||\boldsymbol{g}||_{[H^{1/2}(\Gamma)]^2} \right).$$

The details can be found in Section III in [10].

Now, in order to establish the convergence of the method, we recall the following well-known approximation operators. First, we introduce the Raviart-Thomas interpolation operator (see [8, 22]), $\Pi_h^k : [H^1(\Omega)]^{2\times 2} \to H_h^{\boldsymbol{\sigma}}$, which given $\boldsymbol{\tau} \in [H^1(\Omega)]^{2\times 2}$, $\Pi_h^k(\boldsymbol{\tau})$ is the only element in $H_h^{\boldsymbol{\sigma}}$ such that:

$$\forall\, \boldsymbol{q} \in [\mathcal{P}_k(e)]^2 : \quad \int_e \Pi_h^k(\boldsymbol{\tau})\boldsymbol{n} \cdot \boldsymbol{q} = \int_e \boldsymbol{\tau}\boldsymbol{n} \cdot \boldsymbol{q}, \quad \forall e \in \partial\mathcal{T}_h, \quad \text{when } k \geq 0, \tag{5}$$

with $\partial\mathcal{T}_h$ denoting the list of *edges* (counted once) induced by $\{\partial T\}_{T\in\mathcal{T}_h}$, and

$$\forall\, \boldsymbol{\rho} \in [\mathcal{P}_{k-1}(T)]^{2\times 2} : \quad \int_T \Pi_h^k(\boldsymbol{\tau}) : \boldsymbol{\rho} = \int_T \boldsymbol{\tau} : \boldsymbol{\rho}, \quad \forall T \in \mathcal{T}_h, \quad \text{when } k \geq 1. \tag{6}$$

The operator Π_h^k satisfies the following approximation properties.

Lemma 1 *There exist constants $\tilde{c}_1, \tilde{c}_2, \tilde{c}_3 > 0$, independent of h, such that for all $T \in \mathcal{T}_h$*

$$\forall\, \boldsymbol{\tau} \in [H^m(\Omega)]^{2\times 2} : \quad ||\boldsymbol{\tau} - \Pi_h^k(\boldsymbol{\tau})||_{[L^2(T)]^{2\times 2}} \leq \tilde{c}_1\, h_T^m\, |\boldsymbol{\tau}|_{[H^m(T)]^{2\times 2}} \quad 1 \leq m \leq k+1 \tag{7}$$

and for all $\boldsymbol{\tau} \in [H^{m+1}(\Omega)]^{2\times 2}$ with $\mathbf{div}(\boldsymbol{\tau}) \in [H^m(\Omega)]^2$,

$$||\mathbf{div}(\boldsymbol{\tau} - \Pi_h^k(\boldsymbol{\tau}))||_{[L^2(T)]^2} \leq \tilde{c}_2\, h_T^m\, |\mathbf{div}(\boldsymbol{\tau})|_{[H^m(T)]^2}, \quad 0 \leq m \leq k+1 \tag{8}$$

and

$$\forall\, \boldsymbol{\tau} \in [H^1(\Omega)]^{2\times 2} : \quad ||\boldsymbol{\tau}\boldsymbol{n} - \Pi_h^k(\boldsymbol{\tau})\boldsymbol{n}||_{[L^2(e)]^2} \leq \tilde{c}_3\, h_e^{1/2}\, ||\boldsymbol{\tau}||_{[H^1(T)]^{2\times 2}} \quad \forall\, e \in \partial\mathcal{T}_h. \tag{9}$$

Proof. See e.g. [8] or [22]. $\square$

Moreover, the operator Π_h^k can also be seen as a bounded linear operator from the larger space $[H^s(\Omega)]^{2\times 2} \cap H(\mathbf{div};\Omega)$ into $H_h^{\boldsymbol{\sigma}}$, for all $s \in (0,1]$ (see, e.g. Theorem 3.16 in [20]). In this situation, the following approximation error estimate holds: There exists $C > 0$, independent of the mesh size, such that

$$||\boldsymbol{\tau} - \Pi_h^k(\boldsymbol{\tau})||_{[L^2(T)]^{2\times 2}} \leq C\, h_T^s \left\{ ||\boldsymbol{\tau}||_{[H^s(T)]^{2\times 2}} + ||\mathbf{div}(\boldsymbol{\tau})||_{[L^2(T)]^2} \right\}, \quad \forall T \in \mathcal{T}_h .$$

Another important property reads as

$$\mathbf{div}(\Pi_h^k(\boldsymbol{\tau})) = P_h^k(\mathbf{div}(\boldsymbol{\tau}))\,, \tag{10}$$

with $P_h^k : [L^2(\Omega)]^2 \to H_h^{\boldsymbol{u}}$ being the L^2-orthogonal projector. This is deriving from (5) and (6). On the other hand, it is well known (see, e.g. [12]) that P_h^k verifies: *For each $\boldsymbol{v} \in [H^m(\Omega)]^2$, with $0 \leq m \leq k+1$, there exists $C > 0$, independent of the mesh size, such that*

$$||\boldsymbol{v} - P_h^k(\boldsymbol{v})||_{[L^2(T)]^2} \leq C\, h_T^m\, |\boldsymbol{v}|_{[H^m(T)]^2}\,, \quad \forall T \in \mathcal{T}_h . \tag{11}$$

With the help of these operators, we are able to prove the convergence of the proposed method. Moreover, the corresponding rate of convergence of the method for these choices of finite element subspaces, is recalled in the next theorem.

Theorem 2 *Let $(\boldsymbol{\sigma}, \boldsymbol{u}) \in \boldsymbol{\Sigma}_0$ and $(\boldsymbol{\sigma}_h, \boldsymbol{u}_h) \in \boldsymbol{\Sigma}_{0,h}$ be the unique solutions to problems* (3) *and* (4)*, respectively. In addition, we assume that $\boldsymbol{\sigma} \in [H^t(\Omega)]^{2\times 2}$, $\mathbf{div}(\boldsymbol{\sigma}) \in [H^t(\Omega)]^2$, $\boldsymbol{u} \in [H^t(\Omega)]^2$, for some $t \in (0, k+1]$. Then, there exists $C > 0$, independent of h, such that there holds*

$$\|(\boldsymbol{\sigma}, \boldsymbol{u}) - (\boldsymbol{\sigma}_h, \boldsymbol{u}_h)\|_{\boldsymbol{\Sigma}} \leq C\, h^t \left(\|\boldsymbol{\sigma}\|_{[H^t(\Omega)]^{2\times 2}} + \|\mathbf{div}(\boldsymbol{\sigma})\|_{[H^t(\Omega)]^2} + \|\boldsymbol{u}\|_{[H^t(\Omega)]^2} \right) .$$

Proof. The proof is a straightforward application of the very well known Babuška-Brezzi theory (cf. Theorem II.1.1 in [19]). It relies on bounding each one of the involved errors, $||\boldsymbol{\sigma} - \boldsymbol{\sigma}_h||_{H(\mathbf{div};\Omega)}$ and $||\boldsymbol{u} - \boldsymbol{u}_h||_{[L^2(\Omega)]^2}$, taking into account the properties of the Raviart-Thomas conforming operator Π_h^k, as well as the standard L^2-orthogonal projection operator P_h^k. We omit further details. $\square$

3 An a posteriori error analysis

In this section, we follow [5] (see also [4]) and develop an a posteriori error analysis for the discrete scheme (4), introducing an appropriate Ritz projection of the error and invoking a non standard quasi Helmholtz decomposition result. First, we introduce some notations and results concerning geometric elements of the triangulation $\mathcal{T}_h$, as well as of the Clément operator.

3.1 Notation and some useful results

Given $T \in \mathcal{T}_h$, we let $E(T)$ be the set of its edges, and let E_h be the set of all edges induced by the triangulation $\mathcal{T}_h$. Then, we write $E_h = E_I \cup E_\Gamma$, where $E_I := \{e \in E_h : e \subseteq \Omega\}$ and $E_\Gamma := \{e \in E_h : e \subseteq \Gamma\}$. Also, for each edge $e \in E_h$, we fix a unit normal vector $\boldsymbol{n}_e := (n_1, n_2)^{\mathtt{t}}$, and let $\boldsymbol{t}_e := (-n_2, n_1)^{\mathtt{t}}$ be the corresponding fixed unit tangential vector along e. From now on, when no confusion arises, we simply write $\boldsymbol{n}$ and $\boldsymbol{t}$ instead of $\boldsymbol{n}_e$ and $\boldsymbol{t}_e$, respectively. In addition, let $\boldsymbol{v}$ and $\boldsymbol{\tau}$ be vectorial - and tensor -valued functions, respectively, that are smooth inside each element $T \in \mathcal{T}_h$. We denote by $(\boldsymbol{v}_{T,e}, \boldsymbol{\tau}_{T,e})$ the restriction of $(\boldsymbol{v}_T, \boldsymbol{\tau}_T)$ to e. Then, given $e \in E_I$, we define the jump of $\boldsymbol{v}$ and $\boldsymbol{\tau}$ at $\boldsymbol{x} \in e$, by

$$[\![\boldsymbol{v}]\!] := \boldsymbol{v}_{T,e} - \boldsymbol{v}_{T',e}\,, \quad [\![\boldsymbol{\tau}]\!] := \boldsymbol{\tau}_{T,e}\boldsymbol{t}_T + \boldsymbol{\tau}_{T',e}\boldsymbol{t}_{T'}\,,$$

where T and T' are the two elements in $\mathcal{T}_h$ sharing the edge $e \in E_I$. On boundary edges $e \in E_\Gamma$, we set $[\![\boldsymbol{\tau}]\!] := \boldsymbol{\tau}_{T,e}\boldsymbol{t}_T$, where $T \in \mathcal{T}_h$ is such that $\partial T \cap e \neq \emptyset$. The duality pairing between $[H^{-1/2}(\partial T)]^2$ and $[H^{1/2}(\partial T)]^2$ with respect to $L^2(\partial T)$- inner product, is denoted by $\langle \cdot, \cdot \rangle_{\partial T}$. We also introduce the broken Sobolev space $H^1(\mathcal{T}_h) := \{v \in L^2(\Omega) : v|_T \in H^1(T),\ \forall T \in \mathcal{T}_h\}$.

Finally, given a smooth scalar field v, a vector valued field $\boldsymbol{v} := (v_1, v_2)^{\mathtt{t}}$ and a tensor valued one $\boldsymbol{\tau} := \begin{pmatrix} \tau_{11} & \tau_{12} \\ \tau_{21} & \tau_{22} \end{pmatrix}$, we define

$$\mathbf{curl}(v) := \begin{pmatrix} \frac{\partial v}{\partial x_2} \\ -\frac{\partial v}{\partial x_1} \end{pmatrix}, \quad \underline{\mathbf{curl}}(\boldsymbol{v}) := \begin{pmatrix} \frac{\partial v_1}{\partial x_2} & -\frac{\partial v_1}{\partial x_1} \\ \frac{\partial v_2}{\partial x_2} & -\frac{\partial v_2}{\partial x_1} \end{pmatrix}, \quad \mathrm{rot}(\boldsymbol{v}) := \frac{\partial v_2}{\partial x_1} - \frac{\partial v_1}{\partial x_2}\,,$$

$$\text{and} \quad \mathbf{rot}(\boldsymbol{\tau}) := \begin{pmatrix} \mathrm{rot}\big((\tau_{11}, \tau_{12})^{\mathtt{t}}\big) \\ \mathrm{rot}\big((\tau_{21}, \tau_{22})^{\mathtt{t}}\big) \end{pmatrix} = \begin{pmatrix} \frac{\partial \tau_{12}}{\partial x_1} - \frac{\partial \tau_{11}}{\partial x_2} \\ \frac{\partial \tau_{22}}{\partial x_1} - \frac{\partial \tau_{21}}{\partial x_2} \end{pmatrix}.$$

We will use the Clément operator $I_h : H^1(\Omega) \to X_h$ (cf. [13]), where $X_h := \{v_h \in H^1(\Omega) : v_h\big|_T \in \mathcal{P}_1(T),\ \forall T \in \mathcal{T}_h\}$. A vector version of I_h, say $\boldsymbol{I}_h : [H^1(\Omega)]^2 \to [X_h]^2$, which is defined componentwise by I_h, is also required. The following lemma establishes the local approximation properties of I_h.

Lemma 3 *There exist constants $\tilde{c}_4, \tilde{c}_5 > 0$, independent of h, such that for all $v \in H^1(\Omega)$ there holds*

$$||v - I_h(v)||_{H^m(T)} \leq \tilde{c}_4\, h_T^{1-m}\, |v|_{H^1(\omega(T))}\,, \quad \forall\, m \in \{0,1\}\,, \forall\, T \in \mathcal{T}_h\,,$$

and

$$||v - I_h(v)||_{L^2(e)} \leq \tilde{c}_5\, h_e^{1/2}\, |v|_{H^1(\omega(e))} \quad \forall\, e \in E_h\,,$$

where $\omega(T) := \cup\{T' \in \mathcal{T}_h : T' \cap T \neq \emptyset\}$, h_e denotes the length of the side $e \in E_h$ and $\omega(e) := \cup\{T' \in \mathcal{T}_h : T' \cap e \neq \emptyset\}$.

Proof. We refer to [13]. $\square$

The following inverse inequality will also be required.

Lemma 4 *Let $\ell, m \in \mathbb{N} \cup \{0\}$ such that $\ell \leq m$. Then, there exists $c > 0$, depending only on k, ℓ, m and the shape regularity of the triangulations, such that for each $T \in \mathcal{T}_h$ there holds*

$$|q|_{H^m(T)} \leq c\, h_T^{\ell-m}\, |q|_{H^\ell(T)}\,, \quad \forall\, q \in \mathcal{P}_k(T)\,. \tag{12}$$

Proof. See Theorem 3.2.6 in [12]. $\square$

3.2 Reliability of the estimator

Let $(\boldsymbol{\sigma}, \boldsymbol{u})$ be the unique solution to problem (3) and assume that the Galerkin scheme (4) has a unique solution, $(\boldsymbol{\sigma}_h, \boldsymbol{u}_h)$. We define the Ritz projection of the error with respect to the inner product on $\boldsymbol{\Sigma}$,

$$\langle(\boldsymbol{\sigma}, \boldsymbol{w}), (\boldsymbol{\tau}, \boldsymbol{v})\rangle_{\boldsymbol{\Sigma}} := (\boldsymbol{\sigma}, \boldsymbol{\tau})_{H(\mathbf{div};\Omega)} + (\boldsymbol{w}, \boldsymbol{v})_{[L^2(\Omega)]^2} \quad \forall\, (\boldsymbol{\sigma}, \boldsymbol{w}), (\boldsymbol{\tau}, \boldsymbol{v}) \in \boldsymbol{\Sigma}\,,$$

as the unique element $(\bar{\boldsymbol{\sigma}}, \bar{\boldsymbol{u}}) \in \boldsymbol{\Sigma}$ such that for all $(\boldsymbol{\tau}, \boldsymbol{v}) \in \boldsymbol{\Sigma}$,

$$\langle(\bar{\boldsymbol{\sigma}}, \bar{\boldsymbol{u}}), (\boldsymbol{\tau}, \boldsymbol{v})\rangle_{\boldsymbol{\Sigma}} = A((\boldsymbol{\sigma} - \boldsymbol{\sigma}_h, \boldsymbol{u} - \boldsymbol{u}_h), (\boldsymbol{\tau}, \boldsymbol{v}))\,. \tag{13}$$

where the global bilinear form $A : \boldsymbol{\Sigma} \times \boldsymbol{\Sigma} \to \mathbb{R}$ arises from the variational formulation (3) after adding its equations, that is

$$A((\boldsymbol{\rho}, \boldsymbol{w}), (\boldsymbol{\tau}, \boldsymbol{v})) := a(\boldsymbol{\rho}, \boldsymbol{\tau}) + b(\boldsymbol{w}, \boldsymbol{\tau}) + b(\boldsymbol{v}, \boldsymbol{\rho}) \qquad \forall (\boldsymbol{\rho}, \boldsymbol{w}),\, (\boldsymbol{\tau}, \boldsymbol{v}) \in \boldsymbol{\Sigma}\,.$$

We remark that the existence and uniqueness of $(\bar{\boldsymbol{\sigma}}, \bar{\boldsymbol{u}}) \in \boldsymbol{\Sigma}$ is guaranteed by the Lax-Milgram Lemma.

It is not difficult to check that the properties of the bilinear forms $a(\cdot,\cdot)$ and $b(\cdot,\cdot)$ imply that $A(\cdot,\cdot)$ satisfies a global inf-sup condition, i.e. there exists $\alpha > 0$ such that

$$\alpha\, ||(\boldsymbol{\zeta}, \boldsymbol{w})||_{\boldsymbol{\Sigma}} \leq \sup_{\theta \neq (\boldsymbol{\tau}, \boldsymbol{v}) \in \boldsymbol{\Sigma}_0} \frac{A((\boldsymbol{\zeta}, \boldsymbol{w}), (\boldsymbol{\tau}, \boldsymbol{v}))}{\|(\boldsymbol{\tau}, \boldsymbol{v})\|_{\boldsymbol{\Sigma}}} \qquad \forall (\boldsymbol{\zeta}, \boldsymbol{w}) \in \boldsymbol{\Sigma}_0\,.$$

This property allows us to bound the error in terms of the solution of its Ritz projection. Indeed, we have

$$\begin{aligned} \alpha\, ||(\boldsymbol{\sigma} - \boldsymbol{\sigma}_h, \boldsymbol{u} - \boldsymbol{u}_h)||_{\boldsymbol{\Sigma}} \quad &\leq \sup_{(\boldsymbol{\tau}, \boldsymbol{v}) \in \boldsymbol{\Sigma}_0} \frac{A((\boldsymbol{\sigma} - \boldsymbol{\sigma}_h, \boldsymbol{u} - \boldsymbol{u}_h), (\boldsymbol{\tau}, \boldsymbol{v}))}{\|(\boldsymbol{\tau}, \boldsymbol{v})\|_{\boldsymbol{\Sigma}}} \\ &\leq \sup_{(\boldsymbol{\tau}, \boldsymbol{v}) \in \boldsymbol{\Sigma}} \frac{A((\boldsymbol{\sigma} - \boldsymbol{\sigma}_h, \boldsymbol{u} - \boldsymbol{u}_h), (\boldsymbol{\tau}, \boldsymbol{v}))}{\|(\boldsymbol{\tau}, \boldsymbol{v})\|_{\boldsymbol{\Sigma}}} \;=\; ||(\bar{\boldsymbol{\sigma}}, \bar{\boldsymbol{u}})||_{\boldsymbol{\Sigma}}\,. \end{aligned} \tag{14}$$

Then, according to (14), and in order to obtain a reliable a posteriori error estimates for the discrete scheme (4), it is enough to bound from above the Ritz projection of the error. To this aim, we establish the following technical result, which can be seen as another version of a *quasi-Helmholtz decomposition* of functions in $H(\mathbf{div};\Omega)$.

Lemma 5 *For each $\boldsymbol{\tau} \in H(\mathbf{div};\Omega)$, there exist $\boldsymbol{\chi} \in [H^1(\Omega)]^2$ and $\boldsymbol{\Phi} \in [H_0^1(\Omega)]^{2\times 2}$, such that*

$$\boldsymbol{\tau} \,=\, \mathbf{curl}(\boldsymbol{\chi}) \,+\, \boldsymbol{\Phi} \,+\, \frac{1}{2}\boldsymbol{d} \otimes (x_1 - a, x_2 - b)^{\mathtt{t}}\,, \tag{15}$$

where $(a,b)^{\mathtt{t}}$ is a fixed point belonging to Ω, and $\boldsymbol{d} := (d_1, d_2)^{\mathtt{t}}$ with $d_i = \frac{1}{|\Omega|}\int_\Omega \operatorname{div}(\boldsymbol{\tau}_i)$, $i = 1,2$, with $\boldsymbol{\tau}_i$ denoting the i-th row of the tensor $\boldsymbol{\tau}$. In addition, there exists $C > 0$, such that

$$|\boldsymbol{\chi}|^2_{[H^1(\Omega)]^2} \,+\, \|\boldsymbol{\Phi}\|^2_{[H^1(\Omega)]^{2\times 2}} \,\leq\, C\,\|\boldsymbol{\tau}\|_{H(\mathbf{div};\Omega)}\,. \tag{16}$$

Proof. We first introduce the space $M := \{\boldsymbol{\zeta} \in H(\mathbf{div};\Omega) \,:\, \forall\, i \in \{1,2\} \,:\, \int_\Omega \operatorname{div}(\boldsymbol{\zeta}_i^{\mathtt{t}}) \,=\, 0\}$. Next, for each $\boldsymbol{\tau} \in H(\mathbf{div};\Omega)$, we decompose $\mathbf{div}(\boldsymbol{\tau}) = \mathbf{div}(\tilde{\boldsymbol{\tau}}) + \boldsymbol{d}$. We remark that $\forall\, i \in \{1,2\}$: $\|\operatorname{div}(\boldsymbol{\tau}_i^{\mathtt{t}})\|^2_{0,\Omega} = \|\operatorname{div}(\tilde{\boldsymbol{\tau}}_i^{\mathtt{t}})\|^2_{0,\Omega} + |d_i|^2$. Then, since $\mathbf{div}(\tilde{\boldsymbol{\tau}}) \in [L_0^2(\Omega)]^2$, band invoking Corollary I.2.4 in [19], there exists $\boldsymbol{\Phi} \in [H_0^1(\Omega)]^{2\times 2}$ such that $\mathbf{div}(\boldsymbol{\Phi}) = \mathbf{div}(\tilde{\boldsymbol{\tau}})$ in Ω and $\|\boldsymbol{\Phi}\|_{1,\Omega} \,\leq\, c\,\|\mathbf{div}(\boldsymbol{\tau})\|_{0,\Omega}$. This implies for each $i = 1,2$ that

$$\operatorname{div}\left(\boldsymbol{\tau}_i^{\mathtt{t}} - \boldsymbol{\Phi}_i^{\mathtt{t}} - \frac{d_i}{2}(x_1 - a, x_2 - b)^t\right) = 0 \quad \text{in} \quad \Omega \quad \text{and} \quad \left\langle \left(\boldsymbol{\tau}_i^{\mathtt{t}} - \boldsymbol{\Phi}_i^{\mathtt{t}} - \frac{d_i}{2}(x_1 - a, x_2 - b)^t\right)\cdot \boldsymbol{n}, 1\right\rangle_\Gamma = 0\,,$$

where $(a,b)^{\mathtt{t}}$ is a fixed point belonging to Ω. Hence, by Theorem I.3.1 in [19], for each $i = 1,2$, there exists a stream function $\chi_i \in H^1(\Omega)$ such that $\boldsymbol{\tau}_i^{\mathtt{t}} - \boldsymbol{\Phi}_i^{\mathtt{t}} - \frac{d_i}{2}(x_1 - a, x_2 - b)^t = \mathbf{curl}(\chi_i)$ in Ω. Then, we set the vector $\boldsymbol{\chi} := (\chi_1, \chi_2)^{\mathtt{t}} \in [H^1(\Omega)]^2$, which verifies

$$\begin{aligned}
|\boldsymbol{\chi}|^2_{[H^1(\Omega)]^2} \,=\, ||\operatorname{curl}(\boldsymbol{\chi})||^2_{L^2(\Omega)} \,&=\, \sum_{i=1}^2 \left\|\boldsymbol{\tau}_i^{\mathtt{t}} - \boldsymbol{\Phi}_i^{\mathtt{t}} - \frac{d_i}{2}(x_1 - a, x_2 - b)^{\mathtt{t}}\right\|^2_{L^2(\Omega)} \\
&\leq 2\sum_{i=1}^2 \left(||\boldsymbol{\tau}_i^{\mathtt{t}}||^2_{[L^2(\Omega)]^2} \,+\, ||\boldsymbol{\Phi}_i^{\mathtt{t}}||^2_{[L^2(\Omega)]^2} \,+\, \frac{d_i^2}{4}||(x_1 - a, x_2 - b)||^2_{[L^2(\Omega)]^2}\right) \\
&\leq 2\sum_{i=1}^2 \left(||\boldsymbol{\tau}_i^{\mathtt{t}}||^2_{[L^2(\Omega)]^2} \,+\, ||\boldsymbol{\Phi}_i^{\mathtt{t}}||^2_{[L^2(\Omega)]^2} \,+\, \frac{d_i^2}{4}\big(\operatorname{diam}(\Omega)\big)^2\,|\Omega|\right) \\
&\leq 2\,\max\left\{1, c^2 + \frac{|\Omega|}{4}\big(\operatorname{diam}(\Omega)\big)^2\right\}\,||\boldsymbol{\tau}||^2_{H(\mathbf{div};\Omega)}\,.
\end{aligned}$$

As a result, we establish (16), and we end the proof. $\square$

In what follows, we introduce $\boldsymbol{\chi}_h := (\chi_{1,h}, \chi_{2,h})^{\mathtt{t}}$, with $\chi_{i,h} := I_h(\chi_i)$, $i = 1,2$. This allows us to define a *discrete quasi Helmholtz decomposition* of $\boldsymbol{\tau}$, which is given by

$$\boldsymbol{\tau}_h \,:=\, \mathbf{curl}(\boldsymbol{\chi}_h) \,+\, \Pi_h^r\big(\boldsymbol{\Phi}\big) \,+\, \frac{1}{2}\boldsymbol{d} \otimes (x_1 - a, x_2 - b)^{\mathtt{t}} \,\in\, H_h^{\boldsymbol{\sigma}}\,. \tag{17}$$

Then, we observe that

$$\boldsymbol{\tau} - \boldsymbol{\tau}_h \,=\, \underline{\mathbf{curl}}(\boldsymbol{\chi} - \boldsymbol{\chi}_h) \,+\, \boldsymbol{\Phi} - \Pi_h^r(\boldsymbol{\Phi})\,, \tag{18}$$

which yields

$$\mathbf{div}(\boldsymbol{\tau} - \boldsymbol{\tau}_h) \,=\, \mathbf{div}(\boldsymbol{\Phi} - \Pi_h^r(\boldsymbol{\Phi}))\,. \tag{19}$$

On the other hand, we notice that for each $\tilde{\lambda} \in \mathbb{R}$, we have $A((\boldsymbol{\sigma} - \boldsymbol{\sigma}_h, \boldsymbol{u} - \boldsymbol{u}_h), (\tilde{\lambda}\boldsymbol{I}\,, 0)) = 0$. Then, since each $\boldsymbol{\zeta}_h \in H_h^{\boldsymbol{\sigma}}$ can be decompose as $\boldsymbol{\zeta}_h = \tilde{\boldsymbol{\zeta}}_h + \lambda\boldsymbol{I}$, with $\tilde{\boldsymbol{\zeta}}_h \in H_{0,h}^{\boldsymbol{\sigma}}$ and $\lambda \in \mathbb{R}$, it is not difficult to establish the following orthogonality relation

$$A((\boldsymbol{\sigma} - \boldsymbol{\sigma}_h, \boldsymbol{u} - \boldsymbol{u}_h), (\boldsymbol{\zeta}_h, \boldsymbol{v}_h)) = 0\,, \quad \forall\, (\boldsymbol{\zeta}_h, \boldsymbol{v}_h) \in \boldsymbol{\Sigma}_h := H_h^{\boldsymbol{\sigma}} \times H_h^{u}\,. \tag{20}$$

This latter remark will be useful in our next aim, which consists in deriving an upper bound for $||(\bar{\boldsymbol{\sigma}}, \bar{\boldsymbol{u}})||_{\boldsymbol{\Sigma}}$ in terms of residuals. In order to do that, first, for each $(\boldsymbol{\tau}, \boldsymbol{v}) \in \boldsymbol{\Sigma}$, we denote its induced discrete pair by $(\boldsymbol{\tau}_h, 0) \in \boldsymbol{\Sigma}_h$, where each row of $\boldsymbol{\tau}_h$ is defined in (17). We take into account (20) with $(\boldsymbol{\zeta}_h, \boldsymbol{v}_h) = (\boldsymbol{\tau}_h, \boldsymbol{0})$ and that $(\boldsymbol{\sigma}, \boldsymbol{u})$ is the unique solution for problem (3) to obtain

$$\begin{aligned}
\langle(\bar{\boldsymbol{\sigma}}, \bar{\boldsymbol{u}}), (\boldsymbol{\tau}, \boldsymbol{v})\rangle_{\boldsymbol{\Sigma}} &= A((\boldsymbol{\sigma} - \boldsymbol{\sigma}_h, \boldsymbol{u} - \boldsymbol{u}_h), (\boldsymbol{\tau} - \boldsymbol{\tau}_h, \boldsymbol{v}))\\
&= A((\boldsymbol{\sigma} - \boldsymbol{\sigma}_h, \boldsymbol{u} - \boldsymbol{u}_h), (\tilde{\boldsymbol{\tau}} - \tilde{\boldsymbol{\tau}}_h, \boldsymbol{v})) + A((\boldsymbol{\sigma} - \boldsymbol{\sigma}_h, \boldsymbol{u} - \boldsymbol{u}_h), ((\lambda - \lambda_h)\boldsymbol{I}, \boldsymbol{0}))\\
&= \langle(\boldsymbol{\tau} - \boldsymbol{\tau}_h)\,\boldsymbol{n}, \boldsymbol{g}\rangle - \int_\Omega \left(\frac{1}{2}\tilde{f}\boldsymbol{I}\right) : (\boldsymbol{\tau} - \boldsymbol{\tau}_h) - \int_\Omega \boldsymbol{f}\cdot\boldsymbol{v} - A((\boldsymbol{\sigma}_h, \boldsymbol{u}_h), (\boldsymbol{\tau} - \boldsymbol{\tau}_h, \boldsymbol{v}))\\
&\quad - (\lambda - \lambda_h)\int_\Gamma \boldsymbol{g}\cdot\boldsymbol{n} + \int_\Omega \left(\frac{1}{2}\tilde{f}\boldsymbol{I}\right) : (\lambda - \lambda_h)\boldsymbol{I} + A((\boldsymbol{\sigma}_h, \boldsymbol{u}_h), ((\lambda - \lambda_h)\boldsymbol{I}, \boldsymbol{0}))\,,
\end{aligned} \tag{21}$$

where in the last equality we have taken into account that $\boldsymbol{\tau} - \boldsymbol{\tau}_h = \tilde{\boldsymbol{\tau}} - \tilde{\boldsymbol{\tau}}_h + (\lambda - \lambda_h)\boldsymbol{I}$, with $\tilde{\boldsymbol{\tau}} - \tilde{\boldsymbol{\tau}}_h \in H_0$ and $(\lambda - \lambda_h) \in \mathbb{R}$. Now, recalling the assumptions on $\tilde{f}$ and $\boldsymbol{g}$, we find that

$$A((\boldsymbol{\sigma}_h, \boldsymbol{u}_h), ((\lambda - \lambda_h)\boldsymbol{I}, \boldsymbol{0})) = \int_\Omega \boldsymbol{u}_h \cdot \mathbf{div}\big((\lambda - \lambda_h)\boldsymbol{I}\big) = 0$$

$$-(\lambda - \lambda_h)\int_\Gamma \boldsymbol{g}\cdot\boldsymbol{n} + \int_\Omega \left(\frac{1}{2}\tilde{f}\boldsymbol{I}\right) : (\lambda - \lambda_h)\boldsymbol{I} = -(\lambda - \lambda_h)\left(\langle\boldsymbol{g}\cdot\boldsymbol{n}, 1\rangle - \int_\Omega \tilde{f}\right) = 0\,,$$

and then (21) reduces to

$$\langle(\bar{\boldsymbol{\sigma}}, \bar{\boldsymbol{u}}), (\boldsymbol{\tau}, \boldsymbol{v})\rangle_{\boldsymbol{\Sigma}} = \langle(\boldsymbol{\tau} - \boldsymbol{\tau}_h)\,\boldsymbol{n}, \boldsymbol{g}\rangle + \int_\Omega \left(-\frac{1}{2}\tilde{f}\boldsymbol{I}\right) : (\boldsymbol{\tau} - \boldsymbol{\tau}_h) - \int_\Omega \boldsymbol{f}\cdot\boldsymbol{v} - A((\boldsymbol{\sigma}_h, \boldsymbol{u}_h), (\boldsymbol{\tau} - \boldsymbol{\tau}_h, \boldsymbol{v}))\,. \tag{22}$$

We notice that (22) is equivalent to

$$\begin{aligned}
\langle\bar{\boldsymbol{\sigma}}, \boldsymbol{\tau}\rangle_{H(\mathbf{div};\,\Omega)} &= F_1(\boldsymbol{\tau} - \boldsymbol{\tau}_h)\,, & \forall\,\boldsymbol{\tau} \in H(\mathbf{div};\,\Omega)\,,\\
\langle\bar{\boldsymbol{u}}, \boldsymbol{v}\rangle_{[L^2(\Omega)]^2} &= F_2(\boldsymbol{v})\,, & \forall\,\boldsymbol{v} \in [L^2(\Omega)]^2\,,
\end{aligned}$$

where $F_1 : H(\mathbf{div};\,\Omega) \to \mathbb{R}$ and $F_2 : [L^2(\Omega)]^2 \to \mathbb{R}$ are the bounded linear functionals defined as

$$F_1(\boldsymbol{\rho}) := \langle\boldsymbol{\rho}\,\boldsymbol{n}, \boldsymbol{g}\rangle - \int_\Omega \left(\frac{1}{2}\tilde{f}\boldsymbol{I} + \frac{1}{\nu}\boldsymbol{\sigma}_h^{\mathtt{d}}\right) : \boldsymbol{\rho} - \int_\Omega \boldsymbol{u}_h\cdot\mathbf{div}(\boldsymbol{\rho}) \quad \forall\,\boldsymbol{\rho} \in H(\mathbf{div};\,\Omega)\,,$$

$$F_2(\boldsymbol{w}) := -\int_\Omega (\boldsymbol{f} + \mathbf{div}(\boldsymbol{\sigma}_h))\cdot\boldsymbol{w} \quad \forall\,\boldsymbol{w} \in [L^2(\Omega)]^2\,.$$

Hence, taking into account (18) and (19) we can rewrite $F_1(\boldsymbol{\tau} - \boldsymbol{\tau}_h)$ as follows

$$F_1(\boldsymbol{\tau} - \boldsymbol{\tau}_h) \,=\, R_1(\boldsymbol{\Phi}) \,+\, R_2(\boldsymbol{\chi})\,,$$

where

$$\begin{aligned} R_1(\boldsymbol{\Phi}) \,&:= \langle(\boldsymbol{\Phi} - \Pi_h^k(\boldsymbol{\Phi}))\,\boldsymbol{n}, \boldsymbol{g} - \boldsymbol{u}_h\rangle \,-\, \int_\Omega \left(\frac{1}{\nu}\boldsymbol{\sigma}_h^{\mathtt{d}} - \nabla_h \boldsymbol{u}_h \,+\, \frac{1}{2}\tilde{f}\boldsymbol{I}\right) \,:\, \big(\boldsymbol{\Phi} - \Pi_h^k(\boldsymbol{\Phi})\big) \\ &\quad + \sum_{T\,\in\,\mathcal{T}_h} \int_{\partial T \cap E_I} \boldsymbol{u}_h \cdot \big(\boldsymbol{\Phi} - \Pi_h^k(\boldsymbol{\Phi})\big)\boldsymbol{n}\,, \\ R_2(\boldsymbol{\chi}) \,&:= \,-\int_\Omega \left(\frac{1}{\nu}\boldsymbol{\sigma}_h^{\mathtt{d}} + \frac{1}{2}\tilde{f}\boldsymbol{I}\right) : \underline{\mathbf{curl}}(\boldsymbol{\chi} - \boldsymbol{\chi}_h) \,+\, \langle \underline{\mathbf{curl}}\big(\boldsymbol{\chi} - \boldsymbol{\chi}_h\big)\boldsymbol{n}, \boldsymbol{g}\rangle\,. \end{aligned}$$

Our aim now is to obtain upper bounds for each one of the terms $F_2(\boldsymbol{w})$, $R_1(\boldsymbol{\Phi})$ and $R_2(\boldsymbol{\chi})$.

Lemma 6 *For any $\boldsymbol{w} \in [L^2(\Omega)]^2$, there holds*

$$|F_2(\boldsymbol{w})| \,\le\, \Big(\sum_{T\,\in\,\mathcal{T}_h} \|\boldsymbol{f} + \mathbf{div}(\boldsymbol{\sigma}_h)\|^2_{[L^2(T)]^2}\Big)^{1/2} \|\boldsymbol{w}\|_{[L^2(\Omega)]^2}\,.$$

Proof. The proof follows from a straightforward application of Cauchy-Schwarz inequality. □

Lemma 7 *There exists $C > 0$, independent of h, such that*

$$\begin{aligned} |R_1(\boldsymbol{\Phi})| \,\le C\Bigg(&\sum_{e\,\in\,E_I} h_e\,\|[\![\boldsymbol{u}_h]\!]\|^2_{[L^2(e)]^2} \,+\, \sum_{T\,\in\,\mathcal{T}_h} h_T^2 \left\|\frac{1}{\nu}\boldsymbol{\sigma}_h^{\mathtt{d}} - \nabla \boldsymbol{u}_h + \frac{1}{2}\tilde{f}\boldsymbol{I}\right\|^2_{[L^2(T)]^{2\times 2}} \\ &+ \sum_{e\in E_\Gamma} h_e\,||\boldsymbol{g} - \boldsymbol{u}_h||^2_{[L^2(e)]^2}\Bigg)^{1/2} \|\boldsymbol{\tau}\|_{H(\mathbf{div};\,\Omega)}\,. \end{aligned}$$

Proof. It is a slight modification of Lemma 3.5 in [6]. We omit further details. □

Lemma 8 *Assuming that $\tilde{f} \in H^1(\mathcal{T}_h)$ and $\boldsymbol{g} \in [H^1(\Gamma)]^2$, there exists $C > 0$, independent of h, such that*

$$\begin{aligned} |R_2(\boldsymbol{\chi})| \,\le C \Bigg(&\sum_{T\,\in\,\mathcal{T}_h} h_T^2 \left\|\mathbf{rot}\left(\frac{1}{\nu}\boldsymbol{\sigma}_h^{\mathtt{d}} + \frac{1}{2}\tilde{f}\boldsymbol{I}\right)\right\|^2_{[L^2(T)]^2} \,+ \sum_{e\,\in\,E_I} h_e \left\|\left[\!\!\left[\frac{1}{\nu}\boldsymbol{\sigma}_h^{\mathtt{d}} + \frac{1}{2}\tilde{f}\boldsymbol{I}\right]\!\!\right]\right\|^2_{L^2(e)} \\ &+ \sum_{e\in E_\Gamma} h_e \left\|\left(\frac{1}{\nu}\boldsymbol{\sigma}_h^{\mathtt{d}} + \frac{1}{2}\tilde{f}\boldsymbol{I}\right)\boldsymbol{t} \,-\, \frac{d\boldsymbol{g}}{d\boldsymbol{t}}\right\|^2_{[L^2(e)]^2}\Bigg)^{1/2} \|\boldsymbol{\tau}\|_{H(\mathbf{div};\,\Omega)}\,. \end{aligned}$$

Proof. Integrating by parts, we deduce

$$
\begin{aligned}
R_2(\boldsymbol{\chi}) &= \sum_{T\in\mathcal{T}_h} -\int_T \left(\frac{1}{\nu}\boldsymbol{\sigma}_h^{\mathtt{d}} + \frac{1}{2}\tilde{f}\boldsymbol{I}\right) : \underline{\mathbf{curl}}(\boldsymbol{\chi}-\boldsymbol{\chi}_h) + \langle \underline{\mathbf{curl}}(\boldsymbol{\chi}-\boldsymbol{\chi}_h)\boldsymbol{n}, \boldsymbol{g}\rangle \\
&= \sum_{T\in\mathcal{T}_h} \left\{ -\int_T \mathbf{rot}\left(\frac{1}{\nu}\boldsymbol{\sigma}_h^{\mathtt{d}} + \frac{1}{2}\tilde{f}\boldsymbol{I}\right)\cdot(\boldsymbol{\chi}-\boldsymbol{\chi}_h) + \left\langle \boldsymbol{\chi}-\boldsymbol{\chi}_h, \left(\frac{1}{\nu}\boldsymbol{\sigma}_h^{\mathtt{d}} + \frac{1}{2}\tilde{f}\boldsymbol{I}\right)\boldsymbol{t}\right\rangle_{\partial T} \right\} \\
&\quad - \sum_{e\in E_\Gamma} \int_e \frac{d\boldsymbol{g}}{d\boldsymbol{t}}\,(\boldsymbol{\chi}-\boldsymbol{\chi}_h) \\
&= \sum_{T\in\mathcal{T}_h} -\int_T \mathbf{rot}\left(\frac{1}{\nu}\boldsymbol{\sigma}_h^{\mathtt{d}} + \frac{1}{2}\tilde{f}\boldsymbol{I}\right)\cdot(\boldsymbol{\chi}-\boldsymbol{\chi}_h) + \sum_{e\in E_I}\int_e (\boldsymbol{\chi}-\boldsymbol{\chi}_h)\cdot \left[\!\left[\frac{1}{\nu}\boldsymbol{\sigma}_h^{\mathtt{d}} + \frac{1}{2}\tilde{f}\boldsymbol{I}\right]\!\right] \\
&\quad + \sum_{e\in E_\Gamma}\int_e (\boldsymbol{\chi}-\boldsymbol{\chi}_h)\left(\left(\frac{1}{\nu}\boldsymbol{\sigma}_h^{\mathtt{d}} + \frac{1}{2}\tilde{f}\boldsymbol{I}\right)\boldsymbol{t} - \frac{d\boldsymbol{g}}{d\boldsymbol{t}}\right).
\end{aligned}
$$

Therefore, the proof is completed applying Lemma 3, the Cauchy-Schwarz inequality, the regularity of the mesh and (16). □

The bound of Ritz projection is exhibited in the following Lemma.

Lemma 9 *Under the assumption that $\tilde{f} \in H^1(\mathcal{T}_h)$ and $\boldsymbol{g}\in[H^1(\Gamma)]^2$, there exists a constant $C>0$, independent of h, such that*

$$
C\,||(\bar{\boldsymbol{\sigma}},\bar{\boldsymbol{u}})||_{\boldsymbol{\Sigma}} \le \eta := \left(\sum_{T\in\mathcal{T}_h}\eta_T^2\right)^{1/2}, \tag{23}
$$

where

$$
\begin{aligned}
\eta_T^2 &:= ||\boldsymbol{f}+\mathbf{div}(\boldsymbol{\sigma}_h)||^2_{[L^2(T)]^2} + h_T^2\left\|\frac{1}{\nu}\boldsymbol{\sigma}_h^{\mathtt{d}} - \nabla\boldsymbol{u}_h + \frac{1}{2}\tilde{f}\boldsymbol{I}\right\|^2_{[L^2(T)]^{2\times2}} + h_T^2\left\|\mathbf{rot}\left(\frac{1}{\nu}\boldsymbol{\sigma}_h^{\mathtt{d}} + \frac{1}{2}\tilde{f}\boldsymbol{I}\right)\right\|^2_{[L^2(T)]^2} \\
&\quad + \sum_{e\in E(T)\cap E_I}\left\{ h_e\,||[\![\boldsymbol{u}_h]\!]||^2_{[L^2(e)]^2} + h_e\left\|\left[\!\left[\frac{1}{\nu}\boldsymbol{\sigma}_h^{\mathtt{d}} + \frac{1}{2}\tilde{f}\boldsymbol{I}\right]\!\right]\right\|^2_{[L^2(e)]^2}\right\} \\
&\quad + \sum_{e\in E(T)\cap E_\Gamma}\left\{ h_e\,||\boldsymbol{g}-\boldsymbol{u}_h||^2_{[L^2(e)]^2} + h_e\left\|\left(\frac{1}{\nu}\boldsymbol{\sigma}_h^{\mathtt{d}} + \frac{1}{2}\tilde{f}\boldsymbol{I}\right)\boldsymbol{t} - \frac{d\boldsymbol{g}}{d\boldsymbol{t}}\right\|^2_{[L^2(e)]^2}\right\}.
\end{aligned} \tag{24}
$$

Proof. It follows from Cauchy-Schwarz inequality and Lemmas 6, 7 and 8. □

The following result establishes that the a posteriori error estimator η is reliable and efficient.

Theorem 10 *Assuming that $\tilde{f} \in H^1(\mathcal{T}_h)$ and $\boldsymbol{g}\in[H^1(\Gamma)]^2$, there exists a positive constant $C_{\mathtt{rel}}$, independent of h, such that*

$$
||(\boldsymbol{\sigma}-\boldsymbol{\sigma}_h, \boldsymbol{u}-\boldsymbol{u}_h)||_{\boldsymbol{\Sigma}} \le C_{\mathtt{rel}}\,\eta\,. \tag{25}
$$

Additionally, there exists $C_{\mathtt{eff}} > 0$, independent of h, such that

$$\eta_T^2 \le C_{\mathtt{eff}} \sum_{\substack{T' \in \mathcal{T}_h \\ e \in E(T) \cap E(T')}} ||(\boldsymbol{\sigma} - \boldsymbol{\sigma}_h, \boldsymbol{u} - \boldsymbol{u}_h)||_{T'} + \mathtt{h.o.t.} \tag{26}$$

with $||(\boldsymbol{\tau}, \boldsymbol{v})||_T^2 := \|\boldsymbol{\tau}\|_{H(\mathbf{div};T)}^2 + \|\boldsymbol{v}\|_{[L^2(T)]^2}^2$, and h.o.t. *is meant for eventual high order terms.*

Proof. The reliability of η (first inequality) follows from (14) and Lemma 9. The efficiency of η (second inequality) is established in the next subsection. We omit further details. $\square$

3.3 Efficiency of the estimator

In this section, we proceeds to establish the local efficiency of the local a posteriori error estimate (26). Since $\boldsymbol{f} = -\mathbf{div}(\boldsymbol{\sigma})$ in Ω and $\frac{1}{\nu}\boldsymbol{\sigma}^{\mathtt{d}} - \nabla \boldsymbol{u} = -\frac{1}{2}\tilde{f}\boldsymbol{I}$ in Ω, we have that

$$||\boldsymbol{f} + \mathbf{div}(\boldsymbol{\sigma}_h)||_{[L^2(T)]^2} = ||\mathbf{div}(\boldsymbol{\sigma} - \boldsymbol{\sigma}_h)||_{[L^2(T)]^2} .$$

To bound the rest of terms in (26), we require some ingredients. First, for any $T \in \mathcal{T}_h$ and any $e \in E(T)$, we introduce ψ_T and ψ_e the well known triangle-bubble and edge-bubble functions. This means that $\psi_T \in \mathcal{P}_3(T)$, $\mathrm{supp}(\psi_T) \subseteq T$, $\psi_T = 0$ on ∂T, and $0 \le \psi_T \le 1$ in T. Analogously, $\psi_e|_T \in \mathcal{P}_2(T)$, $\mathrm{supp}(\psi_e) \subseteq \omega_e := \cup\{T' \in \mathcal{T}_h : e \in E(T)\}$, $\psi_e = 0$ on $\partial\omega_e$, and $0 \le \psi_e \le 1$ in ω_e. In addition, we recall from [23] that, given $k \in \mathbb{N} \cup \{0\}$, there exists an extension operator $L : C(e) \to C(T)$ that verifies $\forall\, p \in \mathcal{P}_k(T) : L(p) \in \mathcal{P}_k(T)$, and $\forall\, q \in \mathcal{P}_k(e) : L(q)|_e = q$. Next result resumes known properties of ψ_T, ψ_e and L, whose proof can be found in [23] (cf. proof of Lemma 4.1).

Lemma 11 *For any triangle T there exists positive constants c_1, c_2, c_3 and c_4, depending only on k and the shape of T, such that for all $p \in \mathcal{P}_k(T)$ and $q \in \mathcal{P}_k(e)$, there hold*

$$||\psi_T\, p||_{L^2(T)}^2 \le ||p||_{L^2(T)}^2 \le c_1\, ||\psi_T^{1/2}\, p||_{L^2(T)}^2 , \tag{27}$$

$$||\psi_e\, q||_{L^2(e)}^2 \le ||q||_{L^2(e)}^2 \le c_2\, ||\psi_e^{1/2}\, q||_{L^2(e)}^2 , \tag{28}$$

$$c_3\, h_e\, ||q||_{L^2(e)}^2 \le ||\psi_e^{1/2}\, L(q)||_{L^2(T)}^2 \le c_4\, h_e\, ||q||_{L^2(e)}^2 . \tag{29}$$

From here on, we assume that $\tilde{f} \in H^1(\mathcal{T}_h)$ and $\boldsymbol{g} \in [H^1(\Gamma)]^2$.

Lemma 12 *There exists $C_1 > 0$, independent of the meshsize such that for any $T \in \mathcal{T}_h$ there holds*

$$h_T \left\| \nu^{-1}\boldsymbol{\sigma}_h^{\mathtt{d}} - \nabla \boldsymbol{u}_h + \frac{1}{2}\tilde{f}\,\boldsymbol{I} \right\|_{[L^2(T)]^{2\times 2}} \le h_T\, \nu^{-1}\, ||\boldsymbol{\sigma}_h^{\mathtt{d}} - \boldsymbol{\sigma}^{\mathtt{d}}||_{[L^2(T)]^{2\times 2}} + \sqrt{2}\, ||\boldsymbol{u} - \boldsymbol{u}_h||_{[L^2(T)]^2} + C_1\, h_T\, ||\tilde{f} - \pi_h^s(\tilde{f})||_{L^2(T)} . \tag{30}$$

Proof. First, for any $T \in \mathcal{T}_h$, we introduce the L^2-projection of $\tilde{f}$ onto $\mathcal{P}_s(T)$, with $s \in \mathbb{Z}_0^+$ at our disposal. Then, after applying triangle inequality, we obtain

$$\left\| \nu^{-1}\boldsymbol{\sigma}_h^{\mathtt{d}} - \nabla \boldsymbol{u}_h + \frac{1}{2}\tilde{f}\,\boldsymbol{I} \right\|_{[L^2(T)]^{2\times 2}} \le \left\| \nu^{-1}\boldsymbol{\sigma}_h^{\mathtt{d}} - \nabla \boldsymbol{u}_h + \frac{1}{2}\pi_h^s(\tilde{f})\,\boldsymbol{I} \right\|_{[L^2(T)]^{2\times 2}} + ||\tilde{f} - \pi_h^s(\tilde{f})||_{L^2(T)}\,. \tag{31}$$

This motivates us to set the polynomial-wise function $\boldsymbol{\rho}_h := \nu^{-1}\boldsymbol{\sigma}_h^{\mathtt{d}} - \nabla \boldsymbol{u}_h + \frac{1}{2}\pi_h^s(\tilde{f})\,\boldsymbol{I}$ in T. Now, invoking (27), we have

$$\begin{aligned} c_1^{-1}\,||\boldsymbol{\rho}_h||^2_{[L^2(T)]^{2\times 2}} &\le ||\psi_T^{1/2}\boldsymbol{\rho}_h||^2_{[L^2(T)]^{2\times 2}} = \int_T \left(\nu^{-1}\boldsymbol{\sigma}_h^{\mathtt{d}} - \nabla \boldsymbol{u}_h + \frac{1}{2}\pi_h^s(\tilde{f})\,\boldsymbol{I} \right) : (\psi_T\,\boldsymbol{\rho}_h) \\ &= \int_T \left(\nu^{-1}\boldsymbol{\sigma}_h^{\mathtt{d}} - \nabla \boldsymbol{u}_h + \frac{1}{2}\tilde{f}\,\boldsymbol{I} \right) : (\psi_T\,\boldsymbol{\rho}_h) + \frac{1}{2}\int_T (\pi_h^s(\tilde{f}) - \tilde{f})\boldsymbol{I} : (\psi_T\,\boldsymbol{\rho}_h)\,. \end{aligned} \tag{32}$$

In order to derive (30), it is enough to bound the first term on the right hand side in (32). Taking into account that $\frac{1}{2}\tilde{f}\,\boldsymbol{I} = \nabla\boldsymbol{u} - \nu^{-1}\boldsymbol{\sigma}^{\mathtt{d}}$, and integrating by parts, it follows

$$\begin{aligned} \int_T \left(\nu^{-1}\boldsymbol{\sigma}_h^{\mathtt{d}} - \nabla \boldsymbol{u}_h + \frac{1}{2}\tilde{f}\,\boldsymbol{I} \right) : (\psi_T\,\boldsymbol{\rho}_h) &= \int_T \nu^{-1}(\boldsymbol{\sigma}_h^{\mathtt{d}} - \boldsymbol{\sigma}^{\mathtt{d}}) : (\psi_T\,\boldsymbol{\rho}_h) + \int_T (\nabla\boldsymbol{u} - \nabla\boldsymbol{u}_h) : (\psi_T\,\boldsymbol{\rho}_h) \\ &= \int_T \nu^{-1}(\boldsymbol{\sigma}_h^{\mathtt{d}} - \boldsymbol{\sigma}^{\mathtt{d}}) : (\psi_T\,\boldsymbol{\rho}_h) - \int_T (\boldsymbol{u} - \boldsymbol{u}_h) \cdot \operatorname{div}(\psi_T\,\boldsymbol{\rho}_h)\,. \end{aligned}$$

The rest of the proof relies on applying Cauchy-Schwarz inequality, the inverse inequality (12) with $\ell = 0, m = 1$, as well as the fact that $0 \le \psi_T \le 1$ in T. We omit further details. $\square$

In order to bound most of the rest of terms that defined η_T^2, from here on we assume that $\tilde{f} \in H^1(\Omega)$.

Lemma 13 *There exists $C_2 > 0$, independent of the meshsize, such that for any $T \in \mathcal{T}_h$ there holds*

$$h_T \left\| \mathbf{rot}\left(\nu^{-1}\boldsymbol{\sigma}_h^{\mathtt{d}} + \frac{1}{2}\tilde{f}\,\boldsymbol{I} \right) \right\|_{[L^2(T)]^2} \le C_2\,\nu^{-1}\,||\boldsymbol{\sigma}^{\mathtt{d}} - \boldsymbol{\sigma}_h^{\mathtt{d}}||_{[L^2(T)]^{2\times 2}} + h_T\,||\nabla(\tilde{f} - \pi_h^s(\tilde{f}))||_{[L^2(T)]^2}\,. \tag{33}$$

Proof. We follow similar ideas than the given in the proof of previous Lemma. Considering $\pi_h^s(\tilde{f})$, we deduce, applying triangle inequality, that

$$\left\| \mathbf{rot}\left(\nu^{-1}\boldsymbol{\sigma}_h^{\mathtt{d}} + \frac{1}{2}\tilde{f}\,\boldsymbol{I} \right) \right\|_{[L^2(T)]^2} \le \left\| \mathbf{rot}\left(\nu^{-1}\boldsymbol{\sigma}_h^{\mathtt{d}} + \frac{1}{2}\pi_h^s(\tilde{f})\,\boldsymbol{I} \right) \right\|_{[L^2(T)]^2} + ||\nabla(\tilde{f} - \pi_h^s(\tilde{f}))||_{[L^2(T)]^2}\,. \tag{34}$$

Then, we define the polynomial-wise function $\boldsymbol{\rho}_h := \mathbf{rot}\left(\nu^{-1}\boldsymbol{\sigma}_h^{\mathtt{d}} + \frac{1}{2}\pi_h^s(\tilde{f})\,\boldsymbol{I} \right)$. Now, applying property (27), we deduce

$$\begin{aligned} c_1^{-1}\,||\boldsymbol{\rho}_h||^2_{[L^2(T)]^2} &\le ||\psi_T^{1/2}\,\boldsymbol{\rho}_h||_{[L^2(T)]^2} = \int_T \mathbf{rot}\left(\nu^{-1}\boldsymbol{\sigma}_h^{\mathtt{d}} + \frac{1}{2}\pi_h^s(\tilde{f})\,\boldsymbol{I} \right) \cdot (\psi_T\,\boldsymbol{\rho}_h) \\ &= \int_T \mathbf{rot}\left(\nu^{-1}\boldsymbol{\sigma}_h^{\mathtt{d}} + \frac{1}{2}\tilde{f}\,\boldsymbol{I} \right) \cdot (\psi_T\,\boldsymbol{\rho}_h) + \frac{1}{2}\int_T \mathbf{rot}((\pi_h^s(\tilde{f}) - \tilde{f})\,\boldsymbol{I}) \cdot (\psi_T\,\boldsymbol{\rho}_h)\,. \end{aligned} \tag{35}$$

Since $\frac{1}{2}\tilde{f}\,\boldsymbol{I} = \nabla\boldsymbol{u} - \nu^{-1}\boldsymbol{\sigma}^{\mathtt{d}}$ and $\mathbf{rot}(\nabla\boldsymbol{u}) = \mathbf{0}$, we first integrate by parts, and then we apply Cauchy-Schwarz, the inverse inequality (12) with $\ell = 0, m = 1$, as well as the fact that $\psi_T = 0$ on ∂T and $0 \le \psi_T \le 1$ in T. As a result, we obtain

$$\begin{aligned}\int_T \mathbf{rot}\left(\nu^{-1}\boldsymbol{\sigma}_h^{\mathtt{d}} + \frac{1}{2}\tilde{f}\,\boldsymbol{I}\right)\cdot(\psi_T\,\boldsymbol{\rho}_h) \,&=\, \int_T \nu^{-1}\mathbf{rot}(\boldsymbol{\sigma}_h^{\mathtt{d}} - \boldsymbol{\sigma}^{\mathtt{d}})\cdot(\psi_T\,\boldsymbol{\rho}_h) \,=\, \int_T(\boldsymbol{\sigma}_h^{\mathtt{d}} - \boldsymbol{\sigma}^{\mathtt{d}}) : \underline{\mathbf{curl}}(\psi_T\,\boldsymbol{\rho}_h)\\
&\le \nu^{-1}\,||\boldsymbol{\sigma}_h^{\mathtt{d}} - \boldsymbol{\sigma}^{\mathtt{d}}||_{[L^2(T)]^{2\times 2}}\,||\underline{\mathbf{curl}}(\psi_T\,\boldsymbol{\rho}_h)||_{[L^2(T)]^{2\times 2}}\\
&= \nu^{-1}\,||\boldsymbol{\sigma}_h^{\mathtt{d}} - \boldsymbol{\sigma}^{\mathtt{d}}||_{[L^2(T)]^{2\times 2}}\,||\nabla(\psi_T\,\boldsymbol{\rho}_h)||_{[L^2(T)]^{2\times 2}}\\
&\le C\,\nu^{-1}\,h_T^{-1}\,||\boldsymbol{\sigma}_h^{\mathtt{d}} - \boldsymbol{\sigma}^{\mathtt{d}}||_{[L^2(T)]^{2\times 2}}\,||\psi_T\,\boldsymbol{\rho}_h||_{[L^2(T)]^2}\\
&\le C\,\nu^{-1}\,h_T^{-1}\,||\boldsymbol{\sigma}_h^{\mathtt{d}} - \boldsymbol{\sigma}^{\mathtt{d}}||_{[L^2(T)]^{2\times 2}}\,||\boldsymbol{\rho}_h||_{[L^2(T)]^2}\,.\end{aligned} \tag{36}$$

Then, using (36) to bound the right hand side in (35), we obtain

$$c_1^{-1}\,||\boldsymbol{\rho}_h||_{[L^2(T)]^2} \,\le\, C\,\nu^{-1}\,h_T^{-1}\,||\boldsymbol{\sigma}_h^{\mathtt{d}} - \boldsymbol{\sigma}^{\mathtt{d}}||_{[L^2(T)]^{2\times 2}} \,+\, \frac{1}{2}||\nabla(\tilde{f} - \pi_h^s(\tilde{f}))||_{[L^2(T)]^2}\,. \tag{37}$$

Finally, (34) yields to

$$h_T\,\left\|\mathbf{rot}\left(\nu^{-1}\boldsymbol{\sigma}_h^{\mathtt{d}} + \frac{1}{2}\tilde{f}\,\boldsymbol{I}\right)\right\|_{[L^2(T)]^2} \le C_2\left(\nu^{-1}\,||\boldsymbol{\sigma}_h^{\mathtt{d}} - \boldsymbol{\sigma}^{\mathtt{d}}||_{[L^2(T)]^{2\times 2}} \,+\, h_T\,||\nabla(\tilde{f} - \pi_h^s(\tilde{f}))||_{[L^2(T)]^2}\right)\,.$$

□

The following result gives us a bound of the jump of $\boldsymbol{u}_h$.

Lemma 14 *There exists $C_3 > 0$, independent of the meshsize, such that for any $e \in E_I$ there holds*

$$h_e^{1/2}\,||[\![\boldsymbol{u}_h]\!]||_{[L^2(e)]^2} \,\le\, C_3\,\left(||\boldsymbol{u} - \boldsymbol{u}_h||_{[L^2(\omega_e)]^2} \,+\, ||\boldsymbol{\sigma} - \boldsymbol{\sigma}_h||_{[L^2(\omega_e)]^{2\times 2}}\right)\,. \tag{38}$$

Proof. Given $e \in E_I$, we introduce $\omega_e := T \cup T'$, where T and T' are the elements in $\mathcal{T}_h$ sharing e. Next, we set $\boldsymbol{w}_h := [\![\boldsymbol{u}_h]\!]$ on e and $\boldsymbol{\rho}_e := \psi_e\,L(\boldsymbol{w}_h)\otimes\boldsymbol{n}_{T,e}$ in ω_e. Now, invoking (28), taking advantage that $[\![\boldsymbol{u}]\!] = \mathbf{0}$ on E_I, and after integrating by parts, we derive

$$\begin{aligned}c_2^{-1}\,||\boldsymbol{w}_h||^2_{[L^2(e)]^2} \,\le\, ||\psi_e^{1/2}\,\boldsymbol{w}_h||_{[L^2(e)]^2} \,&=\, \int_e \psi_e\,L(\boldsymbol{w}_h)\cdot[\![\boldsymbol{u}_h - \boldsymbol{u}]\!] \,=\, \int_e(\psi_e\,L(\boldsymbol{w}_h)\otimes\boldsymbol{n}_{T,e})\,\boldsymbol{n}_{T,e}\cdot[\![\boldsymbol{u}_h - \boldsymbol{u}]\!]\\
&=\, \int_e \boldsymbol{\rho}_e\,\boldsymbol{n}_{T,e}\cdot[\![\boldsymbol{u}_h - \boldsymbol{u}]\!] \,=\, \int_{\omega_e}(\boldsymbol{u}_h - \boldsymbol{u})\cdot\mathrm{div}(\boldsymbol{\rho}_e) \,+\, \int_{\omega_e}\nabla_h(\boldsymbol{u}_h - \boldsymbol{u}) : \boldsymbol{\rho}_e\,.\end{aligned} \tag{39}$$

Knowing that for each $T \in \omega_e$

$$\nabla(\boldsymbol{u}_h - \boldsymbol{u}) \,=\, \nu^{-1}(\boldsymbol{\sigma}_h^{\mathtt{d}} \,-\, \boldsymbol{\sigma}^{\mathtt{d}}) \,-\, \left(\nu^{-1}\,\boldsymbol{\sigma}_h^{\mathtt{d}} \,-\, \nabla\boldsymbol{u}_h \,+\, \frac{1}{2}\tilde{f}\,\boldsymbol{I}\right)\,,$$

we deduce that

$$||\nabla(\boldsymbol{u}_h - \boldsymbol{u})||_{[L^2(T)]^{2\times 2}} \,\le\, \nu^{-1}\,||\boldsymbol{\sigma}_h^{\mathtt{d}} \,-\, \boldsymbol{\sigma}^{\mathtt{d}}||_{[L^2(T)]^{2\times 2}} \,+\, \left\|\nu^{-1}\,\boldsymbol{\sigma}_h^{\mathtt{d}} \,-\, \nabla\boldsymbol{u}_h \,+\, \frac{1}{2}\tilde{f}\,\boldsymbol{I}\right\|_{[L^2(T)]^{2\times 2}}\,. \tag{40}$$

On the other hand, taking into account the inverse inequality (12) with $\ell = 0, m = 1$, and the fact that $0 \le \psi_e \le 1$ in ω_e, we deduce

$$\begin{aligned} ||\mathbf{div}(\boldsymbol{\rho}_e)||_{[L^2(T)]^2} &\le \sqrt{2}\,||\nabla\boldsymbol{\rho}_e||_{[L^2(T)]^{2\times 2}} \le c\,\sqrt{2}\,h_T^{-1}\,||\boldsymbol{\rho}_e||_{[L^2(T)]^2} \\ &= c\,\sqrt{2}\,h_T^{-1}\,||\psi_e^{1/2}\,L(\boldsymbol{w}_h)||_{[L^2(T)]^2} \le c\,c_4^{1/2}\,\sqrt{2}\,h_T^{-1/2}\,||\boldsymbol{w}_h||_{[L^2(e)]^2}\,. \end{aligned} \tag{41}$$

Using (41) and (40), we are able to bound the right hand side in (39), and deduce (38). We omit further details. $\square$

For the rest of the proofs, we need to invoke the well known discrete trace inequality, established in Theorem 3.10 in [1] (cf. (2.4) in [2]). This states that there exists $c_5 > 0$, depending only on the shape regularity of the family of triangulations, such that for any $T \in \mathcal{T}_h$ and any $e \in E(T)$, there holds

$$||v||_{L^2(e)} \le c_5\left(h_e^{-1/2}\,||v||_{L^2(T)} + h_e^{1/2}\,||\nabla v||_{[L^2(T)]^2}\right), \quad \forall\, v \in H^1(T)\,. \tag{42}$$

Lemma 15 *There exists $C_4 > 0$, independent of the meshsize, such that for any $e \in E_I$, there holds*

$$\begin{aligned} h_e^{1/2}\left\|\left[\!\left[\nu^{-1}\boldsymbol{\sigma}_h^{\mathtt{d}} + \frac{1}{2}\tilde{f}\,\boldsymbol{I}\right]\!\right]\right\|_{[L^2(e)]^2} &\le C_4\left(\nu^{-1}||\boldsymbol{\sigma}^{\mathtt{d}} - \boldsymbol{\sigma}_h^{\mathtt{d}}||_{[L^2(\omega_e)]^{2\times 2}}\right. \\ &\quad \left. + \sum_{T\in\omega_e} ||\pi_h^s(\tilde{f}) - \tilde{f}||_{L^2(T)} + h_T\,||\nabla(\pi_h^s(\tilde{f}) - \tilde{f})||_{[L^2(T)]^2}\right). \end{aligned} \tag{43}$$

Proof. First, given $e \in E_I$, we apply triangle inequality, and derive

$$\left\|\left[\!\left[\nu^{-1}\boldsymbol{\sigma}_h^{\mathtt{d}} + \frac{1}{2}\tilde{f}\,\boldsymbol{I}\right]\!\right]\right\|_{[L^2(e)]^2} \le \left\|\left[\!\left[\nu^{-1}\boldsymbol{\sigma}_h^{\mathtt{d}} + \frac{1}{2}\pi_h^s(\tilde{f})\,\boldsymbol{I}\right]\!\right]\right\|_{[L^2(e)]^2} + \frac{1}{2}||[\![(\tilde{f} - \pi_h^k(\tilde{f}))\,\boldsymbol{I}]\!]||_{[L^2(e)]^2}\,. \tag{44}$$

This allows us to introduce $\boldsymbol{w}_h := \left[\!\left[\nu^{-1}\boldsymbol{\sigma}_h^{\mathtt{d}} + \frac{1}{2}\pi_h^s(\tilde{f})\,\boldsymbol{I}\right]\!\right]$ on e. Then, taking into account (28), we have

$$\begin{aligned} c_2^{-1}\,||\boldsymbol{w}_h||^2_{[L^2(e)]^2} &\le ||\psi_e^{1/2}\,\boldsymbol{w}_h||^2_{[L^2(e)]^2} = \int_e \psi_e\,L(\boldsymbol{w}_h)\cdot\left[\!\left[\nu^{-1}\boldsymbol{\sigma}_h^{\mathtt{d}} + \frac{1}{2}\pi_h^s(\tilde{f})\,\boldsymbol{I}\right]\!\right] \\ &= \int_e \psi_e\,L(\boldsymbol{w}_h)\cdot\left[\!\left[\nu^{-1}\boldsymbol{\sigma}_h^{\mathtt{d}} + \frac{1}{2}\tilde{f}\,\boldsymbol{I}\right]\!\right] + \frac{1}{2}\int_e \psi_e\,L(\boldsymbol{w}_h)\cdot[\![(\pi_h^s(\tilde{f}) - \tilde{f})\,\boldsymbol{I}]\!]\,. \end{aligned} \tag{45}$$

Our next aim, is to bound the right hand side in (45). We notice that $\nabla\boldsymbol{u} \in H(\mathbf{rot};\Omega)$, to derive

$$\begin{aligned} &\int_e \psi_e\,L(\boldsymbol{w}_h)\cdot\left[\!\left[\nu^{-1}\boldsymbol{\sigma}_h^{\mathtt{d}} + \frac{1}{2}\tilde{f}\,\boldsymbol{I}\right]\!\right] = \int_e \psi_e\,L(\boldsymbol{w}_h)\cdot\left[\!\left[\nu^{-1}\boldsymbol{\sigma}_h^{\mathtt{d}} + \frac{1}{2}\tilde{f}\,\boldsymbol{I} - \nabla\boldsymbol{u}\right]\!\right] \\ &= \int_e \psi_e\,L(\boldsymbol{w}_h)\cdot\left(\nu^{-1}\boldsymbol{\sigma}_h^{\mathtt{d}} + \frac{1}{2}\tilde{f}\,\boldsymbol{I} - \nabla\boldsymbol{u}\right)\boldsymbol{t}_T + \int_e \psi_e\,L(\boldsymbol{w}_h)\cdot\left(\nu^{-1}\boldsymbol{\sigma}_h^{\mathtt{d}} + \frac{1}{2}\tilde{f}\,\boldsymbol{I} - \nabla\boldsymbol{u}\right)\boldsymbol{t}_{T'} \\ &= \sum_{T\in\omega_e}\left\{-\int_T \underline{\mathbf{curl}}(\psi_e\,L(\boldsymbol{w}_h)) : \left(\nu^{-1}\boldsymbol{\sigma}_h^{\mathtt{d}} + \frac{1}{2}\tilde{f}\,\boldsymbol{I} - \nabla\boldsymbol{u}\right) + \int_T \psi_e\,L(\boldsymbol{w}_h)\cdot\mathbf{rot}\left(\nu^{-1}\boldsymbol{\sigma}_h^{\mathtt{d}} + \frac{1}{2}\tilde{f}\,\boldsymbol{I}\right)\right\} \\ &= -\int_{\omega_e} \underline{\mathbf{curl}}(\psi_e\,L(\boldsymbol{w}_h)) : \left(\nu^{-1}\boldsymbol{\sigma}_h^{\mathtt{d}} + \frac{1}{2}\tilde{f}\,\boldsymbol{I} - \nabla\boldsymbol{u}\right) + \int_{\omega_e} \psi_e\,L(\boldsymbol{w}_h)\cdot\mathbf{rot}_h\left(\nu^{-1}\boldsymbol{\sigma}_h^{\mathtt{d}} + \frac{1}{2}\tilde{f}\,\boldsymbol{I}\right). \end{aligned} \tag{46}$$

Then, using in addition the fact that $\nu^{-1}\boldsymbol{\sigma}_h^{\mathtt{d}} + \frac{1}{2}\tilde{f}\,\boldsymbol{I} - \nabla\boldsymbol{u} \,=\, \nu^{-1}(\boldsymbol{\sigma}_h^{\mathtt{d}} - \boldsymbol{\sigma}^{\mathtt{d}})$, (46) reduces to

$$\int_e \psi_e\, L(\boldsymbol{w}_h)\,\cdot\,\left[\!\!\left[\nu^{-1}\boldsymbol{\sigma}_h^{\mathtt{d}} + \frac{1}{2}\tilde{f}\,\boldsymbol{I}\right]\!\!\right] \,=\, \nu^{-1}\int_{\omega_e} \underline{\mathbf{curl}}(\psi_e\, L(\boldsymbol{w}_h))\,:\,(\boldsymbol{\sigma}^{\mathtt{d}} - \boldsymbol{\sigma}_h^{\mathtt{d}}) \\ +\int_{\omega_e} \psi_e\, L(\boldsymbol{w}_h)\,\cdot\,\mathbf{rot}_h\left(\nu^{-1}\boldsymbol{\sigma}_h^{\mathtt{d}} + \frac{1}{2}\tilde{f}\,\boldsymbol{I}\right)\,. \tag{47}$$

Now, for all $T\,\in\,\omega_e$, we have that

$$||\underline{\mathbf{curl}}(\psi_e\, L(\boldsymbol{w}_h))||_{[L^2(T)]^{2\times 2}} \,=\, ||\nabla(\psi_e\, L(\boldsymbol{w}_h))||_{[L^2(T)]^{2\times 2}} \,\le\, c\, h_T^{-1}\, ||\psi_e\, L(\boldsymbol{w}_h)||_{[L^2(T)]^2} \\ \le c\, h_T^{-1}\, ||\psi_e^{1/2}\, L(\boldsymbol{w}_h)||_{[L^2(T)]^2} \,\le\, c\, c_4\, h_T^{-1/2}\, ||\boldsymbol{w}_h||_{[L^2(e)]^2}\,, \tag{48}$$

where we have applied inverse inequality (12) with $\ell = 0, m = 1$, and taken into account the fact that $0\,\le\,\psi_e^{1/2}\,\le 1$ in ω_e, as well as property (28). Moreover, we also derive that

$$||\psi_e\, L(\boldsymbol{w}_h)||_{[L^2(T)]^2} \,\le c_4\, h_T^{1/2}\, ||\boldsymbol{w}_h||_{[L^2(e)]^2}\,, \tag{49}$$

which helps us to obtain

$$\int_e \psi_e\, L(\boldsymbol{w}_h)\,\cdot\,[\![(\pi_h^s(\tilde{f}) - \tilde{f})\,\boldsymbol{I}]\!] \,\le\, ||\boldsymbol{w}_h||_{[L^2(e)]^2}\, ||[\![(\pi_h^s(\tilde{f}) - \tilde{f})\,\boldsymbol{I}]\!]||_{[L^2(e)]^2}\,. \tag{50}$$

Inequalities (48), (49), and (50), together with (33), allow us to deduce from (45) that

$$||\boldsymbol{w}_h||_{[L^2(e)]^2} \,\le C \sum_{T\,\in\,\omega_e} h_T^{-1/2}\nu^{-1}||\boldsymbol{\sigma}^{\mathtt{d}} - \boldsymbol{\sigma}_h^{\mathtt{d}}||_{[L^2(T)]^{2\times 2}} \,+\, ||\pi_h^s(\tilde{f}) - \tilde{f}||_{L^2(e)}\,.$$

Then, it follows from (44), taking into account (42), that

$$h_e^{1/2}\,\left|\left|\left[\!\!\left[\nu^{-1}\boldsymbol{\sigma}_h^{\mathtt{d}} + \frac{1}{2}\tilde{f}\,\boldsymbol{I}\right]\!\!\right]\right|\right|_{[L^2(e)]^2} \,\le C_4\left(\nu^{-1}||\boldsymbol{\sigma}^{\mathtt{d}} - \boldsymbol{\sigma}_h^{\mathtt{d}}||_{[L^2(\omega_e)]^{2\times 2}} \right. \\ \left. +\sum_{T\,\in\,\omega_e} ||\pi_h^s(\tilde{f}) - \tilde{f}||_{L^2(T)} \,+\, h_T\, ||\nabla(\pi_h^s(\tilde{f}) - \tilde{f})||_{[L^2(T)]^2}\right),$$

and we end the proof. □

Next, invoking again the discrete trace inequality (42), and noticing that $\boldsymbol{u} \,=\, \boldsymbol{g}$ on Γ, we are able to establish.

Lemma 16 *There exists $C_5 > 0$, independent of the mesh size, such that for any $e\,\in\,E_\Gamma$, an edge of $T_e \in \mathcal{T}_h$, there holds*

$$h_e^{1/2}\, ||\boldsymbol{g} - \boldsymbol{u}_h||_{[L^2(e)]^2} \,\le\, C_5\,\left(||\boldsymbol{u} - \boldsymbol{u}_h||_{[L^2(T_e)]^2} \,+\, h_{T_e}\,\nu^{-1}\, ||\boldsymbol{\sigma}_h^{\mathtt{d}} - \boldsymbol{\sigma}^{\mathtt{d}}||_{[L^2(T_e)]^{2\times 2}} \,+\, h_{T_e}\, ||\tilde{f} - \pi_h^s(\tilde{f})||_{L^2(T_e)}\right)\,. \tag{51}$$

Proof. Let $e \in E_\Gamma$, and $T_e \in \mathcal{T}_h$ the triangle having e as an edge. Since $\boldsymbol{u} = \boldsymbol{g}$ on e, we have, after applying (42), that

$$\begin{aligned} C^{-1}\, h_e^{1/2}\, ||\boldsymbol{g} - \boldsymbol{u}_h||_{[L^2(e)]^2} &\leq ||\boldsymbol{u} - \boldsymbol{u}_h||_{[L^2(T_e)]^2} + h_{T_e}\, ||\nabla \boldsymbol{u} - \nabla \boldsymbol{u}_h||_{[L^2(T_e)]^{2\times 2}} \\ &\leq ||\boldsymbol{u} - \boldsymbol{u}_h||_{[L^2(T_e)]^2} + h_{T_e}\, \nu^{-1}\, ||\boldsymbol{\sigma}_h^{\mathtt{d}} - \boldsymbol{\sigma}^{\mathtt{d}}||_{[L^2(T_e)]^{2\times 2}} \\ &\quad + h_{T_e} \left\| \nu^{-1}\, \boldsymbol{\sigma}_h^{\mathtt{d}} - \nabla \boldsymbol{u}_h + \frac{1}{2} \tilde{f}\, \boldsymbol{I} \right\|_{[L^2(T_e)]^{2\times 2}}, \end{aligned}$$

where we have invoked (40) in the last bounding. The result is obtained once we use (30). We omit further details. $\square$

Lemma 17 *Assuming in addition that $\boldsymbol{g} \in [H^1(\Gamma)]^2$ is piecewise polynomial, then there exists $C_6 > 0$, independent of the mesh size, such that for any $e \in E_\Gamma$, an edge of $T_e \in \mathcal{T}_h$, there holds*

$$h_e^{1/2} \left\| \left(\frac{1}{\nu} \boldsymbol{\sigma}_h^{\mathtt{d}} + \frac{1}{2} \tilde{f}\, \boldsymbol{I} \right) \boldsymbol{t} - \frac{d\boldsymbol{g}}{d\boldsymbol{t}} \right\|_{[L^2(e)]^2} \leq C_6 \Bigg(\nu^{-1} ||\boldsymbol{\sigma}^{\mathtt{d}} - \boldsymbol{\sigma}_h^{\mathtt{d}}||_{[L^2(T_e)]^{2\times 2}} + ||\tilde{f} - \pi_h^s(\tilde{f})||_{L^2(T_e)} \tag{52}$$

$$+ h_T ||\nabla\big(\tilde{f} - \pi_h^s(\tilde{f})\big)||_{[L^2(T_e)]^2} \Bigg). \tag{53}$$

Proof. Let $e \in E_\Gamma$. By triangle inequality, we have

$$\left\| \left(\frac{1}{\nu} \boldsymbol{\sigma}_h^{\mathtt{d}} + \frac{1}{2} \tilde{f}\, \boldsymbol{I} \right) \boldsymbol{t} - \frac{d\boldsymbol{g}}{d\boldsymbol{t}} \right\|_{[L^2(e)]^2} \leq \left\| \left(\frac{1}{\nu} \boldsymbol{\sigma}_h^{\mathtt{d}} + \frac{1}{2} \pi_h^s(\tilde{f})\, \boldsymbol{I} \right) \boldsymbol{t} - \frac{d\boldsymbol{g}}{d\boldsymbol{t}} \right\|_{[L^2(e)]^2} + \frac{1}{2} ||\big(\tilde{f} - \pi_h^s(\tilde{f})\big)\boldsymbol{t}||_{[L^2(e)]^2}\,. \tag{54}$$

Now, we introduce $\boldsymbol{w}_h := \left(\frac{1}{\nu} \boldsymbol{\sigma}_h^{\mathtt{d}} + \frac{1}{2} \pi_h^s(\tilde{f})\, \boldsymbol{I} \right) \boldsymbol{t} - \frac{d\boldsymbol{g}}{d\boldsymbol{t}}$ on e. Invoking (28), we obtain

$$\begin{aligned} c_2^{-1} ||\boldsymbol{w}_h||^2_{[L^2(e)]^2} \leq ||\psi_e^{1/2} \boldsymbol{w}_h||^2_{[L^2(e)]^2} &= \int_e \psi_e\, \boldsymbol{w}_h \cdot \left(\left(\frac{1}{\nu} \boldsymbol{\sigma}_h^{\mathtt{d}} + \frac{1}{2} \pi_h^s(\tilde{f})\, \boldsymbol{I} \right) \boldsymbol{t} - \frac{d\boldsymbol{g}}{d\boldsymbol{t}} \right) \\ &= \int_e \psi_e\, \boldsymbol{w}_h \cdot \left(\left(\frac{1}{\nu} \boldsymbol{\sigma}_h^{\mathtt{d}} + \frac{1}{2} \tilde{f}\, \boldsymbol{I} \right) \boldsymbol{t} - \frac{d\boldsymbol{g}}{d\boldsymbol{t}} \right) + \frac{1}{2} \int_e \psi_e\, \boldsymbol{w}_h \cdot \big(\pi_h^s(\tilde{f}) - \tilde{f} \big) \boldsymbol{t}\,. \end{aligned} \tag{55}$$

Next, noticing that $\frac{d\boldsymbol{g}}{d\boldsymbol{t}} = (\nabla \boldsymbol{u})\boldsymbol{t}$ on Γ

$$\begin{aligned} &\int_e \psi_e\, \boldsymbol{w}_h \cdot \left(\left(\frac{1}{\nu} \boldsymbol{\sigma}_h^{\mathtt{d}} + \frac{1}{2} \tilde{f}\, \boldsymbol{I} \right) \boldsymbol{t} - \frac{d\boldsymbol{g}}{d\boldsymbol{t}} \right) = \int_{\partial T_e} \psi_e\, L(\boldsymbol{w}_h) \cdot \left(\frac{1}{\nu} \boldsymbol{\sigma}_h^{\mathtt{d}} + \frac{1}{2} \tilde{f}\, \boldsymbol{I} - \nabla \boldsymbol{u} \right) \boldsymbol{t} \\ &= - \int_{T_e} \underline{\mathbf{curl}}\big(\psi_e\, L(\boldsymbol{w}_h)\big) : \left(\nu^{-1} \boldsymbol{\sigma}_h^{\mathtt{d}} + \frac{1}{2} \tilde{f}\, \boldsymbol{I} - \nabla \boldsymbol{u} \right) + \int_{T_e} \psi_e\, L(\boldsymbol{w}_h) \cdot \mathbf{rot} \left(\nu^{-1} \boldsymbol{\sigma}_h^{\mathtt{d}} + \frac{1}{2} \tilde{f}\, \boldsymbol{I} \right). \end{aligned} \tag{56}$$

Since $\nu^{-1}\boldsymbol{\sigma}_h^{\mathtt{d}} + \dfrac{1}{2}\tilde{f}\,\boldsymbol{I} \,-\, \nabla\boldsymbol{u} \,=\, \nu^{-1}\big(\boldsymbol{\sigma}_h^{\mathtt{d}} - \boldsymbol{\sigma}^{\mathtt{d}}\big)$, we derive, after integrating by parts

$$\int_{T_e} \underline{\mathbf{curl}}\big(\psi_e\, L(\boldsymbol{w}_h)\big) \,:\, \left(\nu^{-1}\boldsymbol{\sigma}_h^{\mathtt{d}} + \frac{1}{2}\tilde{f}\,\boldsymbol{I} - \nabla\boldsymbol{u}\right) \,=\, \nu^{-1}\int_{T_e} \underline{\mathbf{curl}}\big(\psi_e\, L(\boldsymbol{w}_h)\big) \,:\, \big(\boldsymbol{\sigma}_h^{\mathtt{d}} - \boldsymbol{\sigma}^{\mathtt{d}}\big)\,.$$

Replacing the latter back in (56), (55) reduces to

$$\begin{aligned} c_2^{-1}||\boldsymbol{w}_h||^2_{[L^2(e)]^2} \,\le\, & \nu^{-1}\int_{T_e} \underline{\mathbf{curl}}\big(\psi_e\, L(\boldsymbol{w}_h)\big) \,:\, \big(\boldsymbol{\sigma}^{\mathtt{d}} - \boldsymbol{\sigma}_h^{\mathtt{d}}\big) \,+\, \int_{T_e} \psi_e\, L(\boldsymbol{w}_h) \,\cdot\, \mathbf{rot}\left(\nu^{-1}\boldsymbol{\sigma}_h^{\mathtt{d}} + \frac{1}{2}\tilde{f}\,\boldsymbol{I}\right) \\ & + \frac{1}{2}\int_e \psi_e\,\boldsymbol{w}_h \,\cdot\, \big(\pi_h^s(\tilde{f}) - \tilde{f}\big)\boldsymbol{t}\,. \end{aligned}$$

Then, applying Cauchy-Schwarz inequality, inverse inequality (12) with $\ell = 0, m = 1$, property (29) and the fact that $0 \,\le\, \psi_e \,\le 1$ in T_e, we obtain

$$\begin{aligned} c_2^{-1}\,||\boldsymbol{w}_h||_{[L^2(e)]^2} \,\le\, C\Bigg(& \nu^{-1}h_{T_e}^{-1/2}\,||\boldsymbol{\sigma}^{\mathtt{d}} - \boldsymbol{\sigma}_h^{\mathtt{d}}||_{[L^2(T_e)]^{2\times 2}} \,+\, h_e^{1/2}\left\|\mathbf{rot}\left(\nu^{-1}\boldsymbol{\sigma}_h^{\mathtt{d}} + \frac{1}{2}\tilde{f}\,\boldsymbol{I}\right)\right\|_{[L^2(T_e)]^2} \\ & +\, ||\pi_h^s(\tilde{f}) - \tilde{f}||_{L^2(e)}\Bigg)\,. \end{aligned} \tag{57}$$

Finally, applying (57) to bound (54), and after invoking (33), we conclude (53) and end the proof. $\square$

4 Numerical experiments

We begin this section by remarking that, for implementation purposes, the null media condition required by the basis of $H_{0,h}^{\boldsymbol{\sigma}}$ can be circumvented by imposing this requirement through a Lagrange multiplier. More precisely, we solve the following auxiliary discrete scheme: Find $(\boldsymbol{\sigma}_h, \boldsymbol{u}_h, \varphi_h) \,\in\, \boldsymbol{\Sigma}_h := H_h^{\boldsymbol{\sigma}} \times H_h^{\boldsymbol{u}} \times \mathbb{R}$ such that

$$\begin{aligned} A((\boldsymbol{\sigma}_h, \boldsymbol{u}_h), (\boldsymbol{\tau}_h, \boldsymbol{v}_h)) \,+\, \varphi_h \int_\Omega \operatorname{tr}(\boldsymbol{\tau}_h) \;&=\; \tilde{G}(\boldsymbol{\tau}_h, \boldsymbol{v}_h)\,, \\ \psi_h \int_\Omega \operatorname{tr}(\boldsymbol{\sigma}_h) \;&=\; 0\,, \end{aligned} \tag{58}$$

for all $(\boldsymbol{\tau}_h, \boldsymbol{v}_h, \psi_h) \,\in\, \boldsymbol{\Sigma}_h$. A standard argument establishes the equivalence between the variational problems (4) and (58). For more details see, for example, Theorem 6.1 in [7].

In what follows, we approximate $\boldsymbol{\sigma}_h$ by elements of $H(\mathbf{div};\Omega)$ that locally belongs to $[\mathrm{RT}_0]^2$ (row-wise), while $\boldsymbol{u}_h$ is looking in $[\mathcal{P}_0(\mathcal{T}_h)]^2$.

Then, we introduce DOF as the total number of degrees of freedom (unknowns) of (58) i.e. $DOF \,:=\, 2 \times$ (Number of edges of $\mathcal{T}_h$) $+\, 2 \times \operatorname{card}(\mathcal{T}_h) + 1$, which leads asymptotically to 4 unknowns per triangle. This reflects the low computational cost of our scheme, almost the same than the required when considering the $\mathcal{P}_1-\text{iso}\mathcal{P}_1$ approximation spaces for the standard velocity-pressure formulation, whose degrees of freedom are asymptotically 4.5 (unknowns) per triangle. In addition, by setting $p_h := \frac{\nu}{2}\pi_h^1(\tilde{f}) - \frac{1}{2}\text{tr}(\boldsymbol{\sigma}_h)$, we obtain a reasonable piecewise linear approximation of the pressure $p = \frac{\nu}{2}\tilde{f} - \frac{1}{2}\text{tr}(\boldsymbol{\sigma})$.

Hereafter, the individual and total errors are denoted as follows

$$\begin{aligned} \boldsymbol{e}(\boldsymbol{u}) &:= \|\boldsymbol{u} - \boldsymbol{u}_h\|_{[L^2(\Omega)]^2}, \quad \boldsymbol{e}(\boldsymbol{\sigma}) := \|\boldsymbol{\sigma} - \boldsymbol{\sigma}_h\|_{H(\mathbf{div},\Omega)}, \\ \boldsymbol{e} &:= \Big([\boldsymbol{e}(\boldsymbol{u})]^2 + [\boldsymbol{e}(\boldsymbol{\sigma})]^2 \Big)^{1/2}, \quad \boldsymbol{e}(p) := \|p - p_h\|_{L^2(\Omega)}, \end{aligned}$$

where $(\boldsymbol{\sigma}, \boldsymbol{u}) \in H_0 \times [H^1(\Omega)]^2$ and $(\boldsymbol{\sigma}_h, \boldsymbol{u}_h) \in H_{0,h}^{\boldsymbol{\sigma}} \times H_h^{\boldsymbol{u}}$ are the unique solutions of the continuous and discrete formulations, respectively. In addition, if $\boldsymbol{e}$ and $\tilde{\boldsymbol{e}}$ stand for the errors at two consecutive triangulations with N and $\tilde{N}$ degrees of freedom, respectively, then the experimental rate of convergence is given by $r := -2\dfrac{\log(\boldsymbol{e}/\tilde{\boldsymbol{e}})}{\log(N/\tilde{N})}$. The definitions of $r(\boldsymbol{u})$, $r(\boldsymbol{\sigma})$, and $r(p)$ are defined analogously. In the next examples, we concentrate in the iterative process to approximate the exact solution using an adaptive algorithm in the mesh refinement based on an estimator η_T. This algorithm reads as follows following (see [24]):

1. Start with a coarse mesh $\mathcal{T}_h$.
2. Solve the Galerkin scheme (58) for the current mesh $\mathcal{T}_h$.
3. Compute η_T (cf. (24)) for each $T \in \mathcal{T}_h$.
4. Consider stopping criterion and decide to finish or go to the next step.
5. Use *Blue-green* procedure to refine each element $T' \in \mathcal{T}_h$ such that
$$\eta_{T'} \geq \frac{1}{2}\max\{\eta_T : T \in \mathcal{T}_h\}.$$
6. Define the resulting mesh as the new $\mathcal{T}_h$ and go to step 2.

4.1 Example 1: Laminar flow, with smooth divergence free solution

In order to exhibit the robustness of our scheme with respect to the viscosity parameter ν, we consider the two-dimensional analytical solution of the Navier-Stokes equations derived by Kovasznay in [21], where the velocity, the pressure and the domain are given by:

$$\boldsymbol{u}(x,y) := \begin{pmatrix} 1 - \mathrm{e}^{\lambda x}\cos(2\pi y) \\ \frac{\lambda}{2\pi}\mathrm{e}^{\lambda x}\sin(2\pi y) \end{pmatrix}, \quad p(x,y) := -\frac{1}{2}\mathrm{e}^{2\lambda x} - p_0, \quad \Omega := (-1/2, 3/2) \times (0,2), \tag{59}$$

where the constant p_0 is chosen to ensure $p \in L_0^2(\Omega)$, while the parameter λ is setting as:

$$\lambda := -\frac{8\pi^2}{\nu^{-1} + \sqrt{\nu^{-2} + 16\pi^2}}.$$

We emphasize that here $\tilde{f} = \operatorname{div}(\boldsymbol{u}) = 0$ in Ω and the solution is smooth. Then, we present the results just for uniform refinement, ranging the viscosity from 1 to 10^{-4}, i.e. for moderate values of the viscosity. Tables 1, 2 and 3 report the convergence histories as well as the respective rates of convergence of individual errors and the total one, considering a sequence of uniform refinements, for $\nu = 1$, $\nu = 10^{-2}$ and $\nu = 10^{-4}$, respectively. Figure 1, in log-log scale, summarizes these results. In each case, we notice that the scheme is convergent, with the expected optimal rate of convergence $\mathcal{O}(h)$, in agreement with Theorem 2. We also notice that the index of efficiency $\mathbf{e}/\eta$ remains bounded, for each one of the values considered for ν.

4.2 Example 2: Non smooth benchmark solution

Here, we take the problem from [24], which is defined in $\Omega := \{(x_1, x_2) \in \mathbb{R}^2 : x_1^2 + x_2^2 < 1\} \setminus [0,1]\times[-1,0]$. The data of this problem is given such that the exact solution, in polar coordinates, is

$$\boldsymbol{u}(r,\theta) := \begin{pmatrix} r^{\lambda}[(1+\lambda)\sin(\theta)\,\psi(\theta) + \cos(\theta)\,\psi'(\theta)] \\ r^{\lambda}[-(1+\lambda)\cos(\theta)\,\psi(\theta) + \sin(\theta)\,\psi'(\theta)] \end{pmatrix} + \begin{pmatrix} r^2\cos^2(\theta) \\ r^2\sin^2(\theta) \end{pmatrix}, \quad \text{and}$$

$$p(r,\theta) := -\frac{r^{\lambda-1}}{1-\lambda}[(1+\lambda^2)\,\psi'(\theta) + \psi'''(\theta)]\,,$$

with

$$\begin{aligned} \psi(\theta) :=& \frac{1}{1+\lambda}\sin((1+\lambda)\theta)\,\cos(\lambda\,\omega) - \cos((1+\lambda)\theta) \\ & - \frac{1}{1-\lambda}\sin((1-\lambda)\theta)\,\cos(\lambda\,\omega) + \cos((1-\lambda)\theta)\,, \\ \lambda :=& \,0.54448373678246\,, \quad \omega := \frac{3}{2}\pi\,. \end{aligned}$$

We remark that $\int_\Omega p = 0$ and $\tilde{f} \neq 0$ in Ω. Moreover, in this case the exact solution $(\boldsymbol{u}, p)$ lives in $[H^{1+\lambda}(\Omega)]^2 \times H^{\lambda}(\Omega)$. The history of convergence of the method is displayed in Table 4, considering sequences of uniform and adaptive refined meshes generated according to the proposed Algorithm. We notice that due to the low regularity of the exact solution, the total error, when applying uniform refinement, behaves as $\mathcal{O}(h^{\lambda})$, which is in agreement with Theorem 2. On the other hand, when performing the adaptive refinement algorithm, based on our a posteriori error estimator η, the quality of approximation is improved, recovering the optimal rate of convergence, as it can be seen in Table 4 and Figure 2 (in log-log scale). In addition, this adaptive procedure is able to identify the singularity of $\boldsymbol{u}$ and p at origin. This is shown in Figure 4, which contains some of the adapted meshes obtained in this process. Concerning the index of efficiency, we observe that their values are bounded, when considering uniformly refined meshes and the sequence of meshes obtained by applying the adaptive refinement algorithm. These let us to state that our a posteriori error estimator η, is reliable and locally efficient, as stated in Theorem 10.

4.3 Example 3: Another non smooth solution

We now specify the data of our third example. We set $\Omega := \{(x_1, x_2) \in \mathbb{R}^2 : x_1^2 + x_2^2 < 1\} \setminus ([0,1] \times [-1,0])$, and consider the data $\tilde{f}$, $\boldsymbol{f}$ and $\boldsymbol{g}$ such that the exact solution $(\boldsymbol{u}, p)$ is given by

$$\boldsymbol{u}(x_1,x_2) := \frac{1}{8\,\pi\,\nu}\left\{-\ln(s)\begin{pmatrix}1\\0\end{pmatrix} + \frac{1}{s^2}\begin{pmatrix}(x_1-2)^2\\(x_1-2)(x_2-2)\end{pmatrix}\right\} + \begin{pmatrix}x_1^2\\x_2^2\end{pmatrix}$$

$$p(\tilde{r},\theta) := \tilde{r}^{2/3}\,\sin\left(\frac{2}{3}\theta\right) - \frac{3}{2\pi}\,,$$

where $s := \sqrt{(x_1-2)^2 + (x_2-2)^2}$, and the pressure p is given in polar coordinates $(\tilde{r},\theta)$. We pointwise that in this case, $\tilde{f} = \operatorname{div}(\boldsymbol{u}) = 2(x_1+x_2)$, and the exact pressure p lives in $H^{1+2/3}(\Omega)$, since their derivatives are singular at $(0,0)$. In Table 5 we report the convergence history of the method, considering uniform and adaptive refinements. Under the sequence of uniform refinement meshes, we notice that the corresponding rate of convergence behaves as $\mathcal{O}(h^{0.75})$, due to the lack of regularity of exact solution. This is still in agreement with Theorem 2. Moreover, we observe that the L^2-norm of the error of the pressure behaves as $\mathcal{O}(h)$, which is better than expected. Now, when we consider a sequence of adaptive refinement meshes in the *proposed Adaptive Refinement Algorithm*, based on η, we improve the quality of the approximation, recovering the optimal rate of convergence $\mathcal{O}(h)$, as can be seen in Table 5 and in Figure 3. In addition, the index of efficiency computed for uniform and adaptive refinement, are bounded, confirming the validity of Theorem 10. Some adapted meshes, generated by this adaptive procedure, are displayed in Figure 5.

dof	$\boldsymbol{e}(\boldsymbol{u})$	$r(\boldsymbol{u})$	$\boldsymbol{e}(\boldsymbol{\sigma})$	$r(\boldsymbol{\sigma})$	$\boldsymbol{e}(p)$	$r(p)$	$\boldsymbol{e}$	r	$\boldsymbol{e}/\eta$
337	0.647e+1	—-	0.315e+3	—-	0.273e+2	—-	0.317e+3	—-	0.8819
1313	0.285e+1	1.2060	0.203e+3	0.6452	0.167e+2	0.7190	0.204e+3	0.6459	0.8238
5185	0.135e+1	1.0860	0.111e+3	0.8831	0.883e+1	0.9325	0.111e+3	0.8835	0.7895
20609	0.663e+0	1.0328	0.568e+2	0.9699	0.442e+1	1.0032	0.570e+2	0.9701	0.7684
82177	0.329e+0	1.0110	0.286e+2	0.9934	0.219e+1	1.0173	0.287e+2	0.9936	0.7570
328193	0.164e+0	1.0035	0.143e+2	0.9990	0.108e+1	1.0132	0.143e+2	0.9990	0.7513
1311745	0.822e-1	1.0012	0.716e+1	1.0000	0.540e+0	1.0070	0.718e+1	1.0001	0.7485
5244929	0.411e-1	1.0004	0.358e+1	1.0002	0.269e+0	1.0030	0.359e+1	1.0002	0.7472

Table 1: History of convergence and corresponding rates of convergence, Example 1, $\nu = 1.0$ (uniform refinement)

5 Conclusion and final comments

In this paper, we have developed an a posteriori error analysis for the Stokes problem with non homogeneous source terms (in particular with $\tilde{f} \neq 0$ in Ω). The system is approximated by a conforming dual mixed technique, which is based on the so-called pseudostress-velocity formulation (see [3]). This

dof	$\boldsymbol{e}(\boldsymbol{u})$	$r(\boldsymbol{u})$	$\boldsymbol{e}(\boldsymbol{\sigma})$	$r(\boldsymbol{\sigma})$	$\boldsymbol{e}(p)$	$r(p)$	$\boldsymbol{e}$	r	$\boldsymbol{e}/\eta$
337	0.104e+1	—-	0.303e+0	—-	0.533e-1	—-	0.108e+1	——	0.0438
1313	0.414e+0	1.3532	0.149e+0	1.0452	0.242e-1	1.1607	0.441e+0	1.3234	0.0275
5185	0.186e+0	1.1667	0.743e-1	1.0086	0.113e-1	1.1110	0.200e+0	1.1467	0.0222
20609	0.894e-1	1.0605	0.372e-1	1.0049	0.540e-2	1.0671	0.970e-1	1.0526	0.0204
82177	0.442e-1	1.0184	0.186e-1	1.0027	0.265e-2	1.0306	0.480e-1	1.0161	0.0198
328193	0.220e-1	1.0054	0.929e-2	1.0013	0.132e-2	1.0116	0.239e-1	1.0048	0.0196
1311745	0.110e-1	1.0016	0.464e-2	1.0006	0.656e-3	1.0041	0.120e-1	1.0015	0.0195
5244929	0.550e-2	1.0006	0.232e-2	1.0003	0.328e-3	1.0014	0.598e-2	1.0005	0.0195

Table 2: History of convergence and corresponding rates of convergence, Example 1, $\nu = 0.01$ (uniform refinement)

dof	$\boldsymbol{e}(\boldsymbol{u})$	$r(\boldsymbol{u})$	$\boldsymbol{e}(\boldsymbol{\sigma})$	$r(\boldsymbol{\sigma})$	$\boldsymbol{e}(p)$	$r(p)$	$\boldsymbol{e}$	r	$\boldsymbol{e}/\eta$
337	0.125e+1	—-	0.349e-2	—-	0.666e-3	—-	0.125e+1	—-	0.0409
1313	0.487e+0	1.3799	0.171e-2	1.0459	0.297e-3	1.1873	0.487e+0	1.3799	0.0250
5185	0.216e+0	1.1881	0.855e-3	1.0098	0.137e-3	1.1235	0.216e+0	1.1881	0.0197
20609	0.103e+0	1.0692	0.428e-3	1.0052	0.657e-4	1.0678	0.103e+0	1.0692	0.0179
82177	0.509e-1	1.0209	0.214e-3	1.0027	0.323e-4	1.0285	0.509e-1	1.0209	0.0174
328193	0.254e-1	1.0060	0.107e-3	1.0013	0.160e-4	1.0102	0.254e-1	1.0060	0.0172
1311745	0.127e-1	1.0018	0.534e-4	1.0006	0.800e-5	1.0035	0.127e-1	1.0018	0.0171
5244929	0.633e-2	1.0006	0.267e-4	1.0003	0.400e-5	1.0012	0.633e-2	1.0006	0.0171

Table 3: History of convergence and corresponding rates of convergence, Example 1, $\nu = 0.0001$ (uniform refinement)

approach is an extension of the classical one, previously introduced in [10, 11], where the study is done assuming the classical incompressibility condition $\mathrm{div}(\boldsymbol{u}) = 0$ in Ω. The analysis developed here requires a nonstandard quasi-Helmholtz decomposition in $H(\mathbf{div}; \Omega)$ (cf. Lemma 5). Moreover, assuming a reasonable additional regularity of the exact solution (for example, $\boldsymbol{u} \in [H^{1+s}(\Omega)]^2$, for some $s > 1/2$), we derive a reliable a posteriori error estimate (cf. (25)). In addition, introducing a suitable approximation of the datum $\tilde{f}$, and assuming that $\boldsymbol{g}$ is a continuous piecewise polynomial on Γ, we are able to establish the local efficiency of the estimator (cf. (26)), up to the presence of an *oscillation term* of $\tilde{f}$, which is expected to be a *high order term* when it is smooth enough.

Furthermore, numerical examples show that our scheme converges and is robust for moderate values of the viscosity ν (cf. Example 1). In addition, when the exact solution is non smooth (cf. Examples 2 and 3), the proposed *Adaptive Refinement Algorithm*, based on η (cf. Theorem 10), is able to localize the singularities of the solution (see Figures 4 and 5 for Examples 2 and 3, respectively). As a consequence, we notice that the quality of approximation is improved, recovering the optimal rate of convergence of the method. Moreover, the index of efficiency in each case remains bounded,

dof	$\boldsymbol{e}(\boldsymbol{u})$	$r(\boldsymbol{u})$	$\boldsymbol{e}(\boldsymbol{\sigma})$	$r(\boldsymbol{\sigma})$	$\boldsymbol{e}(p)$	$r(p)$	$\boldsymbol{e}$	r	$\boldsymbol{e}/\eta$
1015	0.263e+0	—-	0.254e+1	—-	0.155e+1	——	0.299e+1	—-	0.6090
3989	0.133e+0	0.9974	0.158e+1	0.6910	0.918e+0	0.7666	0.183e+1	0.7126	0.5316
15817	0.665e-1	1.0064	0.102e+1	0.6317	0.572e+0	0.6875	0.117e+1	0.6468	0.4975
62993	0.331e-1	1.0077	0.681e+0	0.5907	0.371e+0	0.6250	0.776e+0	0.5997	0.4821
251425	0.165e-1	1.0072	0.459e+0	0.5680	0.247e+0	0.5870	0.522e+0	0.5729	0.4749
1004609	0.822e-2	1.0064	0.313e+0	0.5562	0.167e+0	0.5661	0.354e+0	0.5587	0.4716
dof	$\boldsymbol{e}(\boldsymbol{u})$	$r(\boldsymbol{u})$	$\boldsymbol{e}(\boldsymbol{\sigma})$	$r(\boldsymbol{\sigma})$	$\boldsymbol{e}(p)$	$r(p)$	$\boldsymbol{e}$	r	$\boldsymbol{e}/\eta$
1015	0.263e+0	—-	0.254e+1	—-	0.155e+1	—-	0.299e+1	—-	0.6090
1209	0.236e+0	1.2306	0.183e+1	3.7699	0.107e+1	4.2005	0.213e+1	3.8577	0.4882
1373	0.233e+0	0.2437	0.148e+1	3.2987	0.847e+0	3.7315	0.172e+1	3.3601	0.4194
1903	0.216e+0	0.4523	0.117e+1	1.4644	0.644e+0	1.6840	0.135e+1	1.4940	0.3735
2769	0.199e+0	0.4299	0.927e+0	1.2204	0.492e+0	1.4288	0.107e+1	1.2426	0.3288
4937	0.154e+0	0.8856	0.713e+0	0.9073	0.364e+0	1.0469	0.815e+0	0.9353	0.3113
7925	0.118e+0	1.1421	0.542e+0	1.1622	0.265e+0	1.3362	0.614e+0	1.1950	0.2952
10417	0.107e+0	0.6723	0.457e+0	1.2428	0.217e+0	1.4777	0.517e+0	1.2626	0.2781
16573	0.879e-1	0.8646	0.367e+0	0.9406	0.170e+0	1.0481	0.414e+0	0.9557	0.2694
26823	0.671e-1	1.1216	0.287e+0	1.0250	0.130e+0	1.1192	0.322e+0	1.0448	0.2646
36225	0.585e-1	0.9092	0.242e+0	1.1319	0.108e+0	1.2437	0.271e+0	1.1398	0.2584
53423	0.493e-1	0.8795	0.200e+0	0.9798	0.876e-1	1.0578	0.224e+0	0.9872	0.2528
81727	0.402e-1	0.9608	0.164e+0	0.9421	0.712e-1	0.9802	0.183e+0	0.9488	0.2516
120813	0.322e-1	1.1429	0.134e+0	1.0394	0.577e-1	1.0731	0.149e+0	1.0494	0.2497
173047	0.271e-1	0.9627	0.111e+0	1.0404	0.475e-1	1.0764	0.124e+0	1.0421	0.2472
251237	0.229e-1	0.8861	0.924e-1	0.9767	0.395e-1	0.9973	0.103e+0	0.9753	0.2456
375075	0.185e-1	1.0629	0.761e-1	0.9679	0.325e-1	0.9780	0.848e-1	0.9740	0.2452
556483	0.150e-1	1.0618	0.623e-1	1.0214	0.265e-1	1.0277	0.693e-1	1.0242	0.2451
785543	0.128e-1	0.9505	0.521e-1	1.0308	0.221e-1	1.0495	0.580e-1	1.0297	0.2429

Table 4: History of convergence and corresponding rates of convergence, Example 2 with $\nu = 1.0$ (uniform and adaptive refinements)

showing that our a posteriori error estimator is reliable and locally efficient, despite the fact that in all these examples the datum $\boldsymbol{g}$ is not piecewise polynomial on Γ, as required by Theorem 10. This gives us numerical evidence that this requirement could be circumvented to derive a similar result as Theorem 10. We leave this for a future work.

Acknowledgments. This research was partially supported by ANID-Chile through the project Centro de Modelamiento Matemático (AFB170001) of the PIA Program: Concurso Apoyo a Centros Científicos y Tecnológicos de Excelencia con Financiamiento Basal CONICYT-Chile and by FONDECYT Grant 1200051; by Centro de Investigación en Ingeniería Matemática (CI^{2}MA), Universidad de

dof	$\boldsymbol{e}(\boldsymbol{u})$	$r(\boldsymbol{u})$	$\boldsymbol{e}(\boldsymbol{\sigma})$	$r(\boldsymbol{\sigma})$	$\boldsymbol{e}(p)$	$r(p)$	$\boldsymbol{e}$	r	$\boldsymbol{e}/\eta$
15817	0.196e-1	—-	0.557e-1	—-	0.160e-1	—-	0.612e-1	—-	0.2523
62993	0.982e-2	1.0021	0.311e-1	0.8438	0.789e-2	1.0198	0.336e-1	0.8695	0.2747
251425	0.491e-2	1.0013	0.178e-1	0.8033	0.393e-2	1.0065	0.189e-1	0.8283	0.3073
1004609	0.246e-2	1.0007	0.105e-1	0.7675	0.196e-2	1.0022	0.109e-1	0.7900	0.3513
4016257	0.123e-2	1.0004	0.629e-2	0.7380	0.982e-3	1.0008	0.648e-2	0.7565	0.4074
dof	$\boldsymbol{e}(\boldsymbol{u})$	$r(\boldsymbol{u})$	$\boldsymbol{e}(\boldsymbol{\sigma})$	$r(\boldsymbol{\sigma})$	$\boldsymbol{e}(p)$	$r(p)$	$\boldsymbol{e}$	r	$\boldsymbol{e}/\eta$
15817	0.196e-1	—-	0.557e-1	—-	0.160e-1	—-	0.612e-1	—-	0.2523
16259	0.194e-1	0.9891	0.505e-1	7.1475	0.158e-1	0.8608	0.563e-1	6.0074	0.2343
34919	0.138e-1	0.8833	0.381e-1	0.7351	0.122e-1	0.6747	0.423e-1	0.7468	0.2386
59423	0.104e-1	1.0790	0.280e-1	1.1612	0.883e-2	1.2142	0.311e-1	1.1566	0.2384
71625	0.957e-2	0.8624	0.252e-1	1.1242	0.808e-2	0.9448	0.281e-1	1.0799	0.2318
145943	0.688e-2	0.9285	0.190e-1	0.7999	0.614e-2	0.7727	0.211e-1	0.8119	0.2339
239707	0.524e-2	1.0931	0.143e-1	1.1299	0.455e-2	1.2072	0.159e-1	1.1324	0.2345
308913	0.473e-2	0.8144	0.125e-1	1.0789	0.401e-2	0.9918	0.139e-1	1.0422	0.2280
589989	0.345e-2	0.9701	0.958e-2	0.8212	0.309e-2	0.8085	0.106e-1	0.8366	0.2311
971111	0.264e-2	1.0785	0.725e-2	1.1193	0.230e-2	1.1819	0.805e-2	1.1201	0.2315
1280317	0.235e-2	0.8351	0.623e-2	1.0966	0.199e-2	1.0369	0.695e-2	1.0627	0.2253
2374931	0.173e-2	0.9923	0.481e-2	0.8364	0.154e-2	0.8338	0.534e-2	0.8533	0.2288
3914411	0.133e-2	1.0699	0.364e-2	1.1153	0.115e-2	1.1617	0.404e-2	1.1143	0.2291

Table 5: History of convergence and corresponding rates of convergence, Example 3 with $\nu = 1.0$ (uniform and adaptive refinements)

Concepción (Chile), and by Dirección de Investigación de la Universidad Católica de la Santísima Concepción (Chile), through Incentivo Mensual program. All authors have contributed equally in this article.

References

[1] S. Agmon, Lectures on Elliptic Boundary Value Problems. Van Nostrand, Princeton, New Jersey, 1965.

[2] D.N. Arnold, *An interior penalty finite element method with discontinuous elements.* SIAM Journal on Numerical Analysis, vol. 19, 4, pp. 742-760, (1982).

[3] T. P. Barrios, E. M. Behrens and R. Bustinza. *A stabilized mixed method applied to Stokes system with nonhomogeneous source terms: The stationary case.* International Journal for Numerical Methods in Fluids, vol 92, pp. 509-527, (2020).

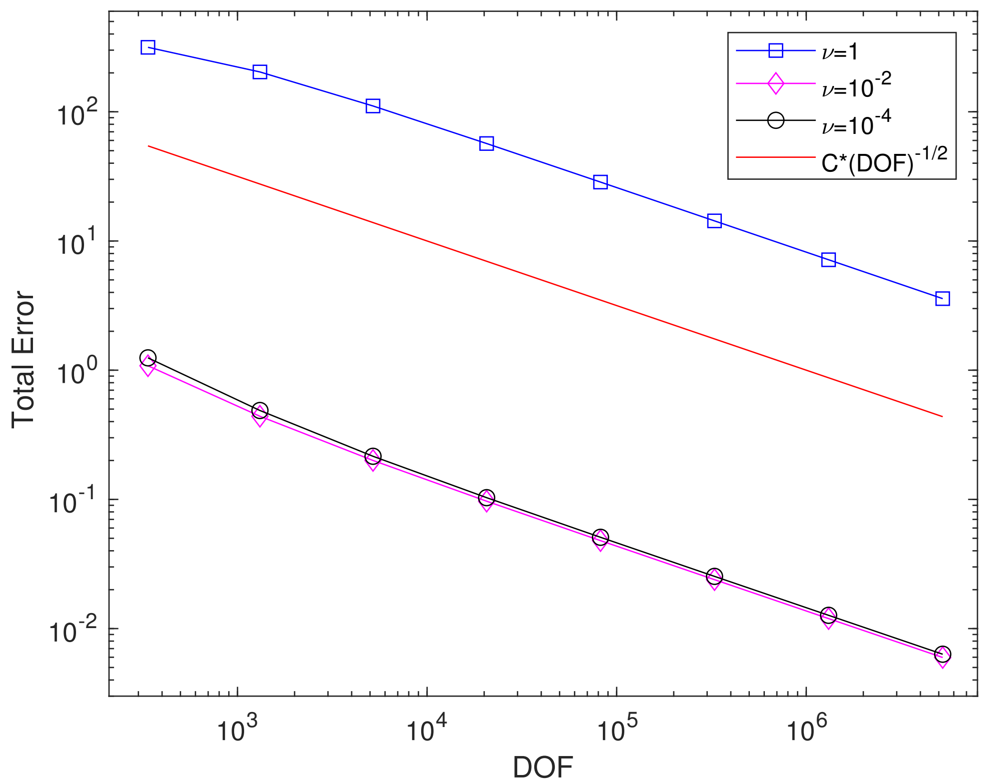

Figure 1: Total error ($\boldsymbol{e}$) vs DOF (N) for uniform and adaptive refinements (Example 1, with $\nu \in \{1, 10^{-2}, 10^{-4}\}$)

[4] T. P. Barrios, E. M. Behrens and M. González. *Low cost A posteriori error estimators for an augmented mixed FEM in linear elasticity*. Applied Numerical Mathematics, vol. 84, pp. 46-65, (2014).

[5] T. P. Barrios, R. Bustinza and C. Campos . *A note on a posteriori error estimate for dual mixed method*. Preprint 2020-08, Departamento de Ingeniería Matemática, Universidad de Concepción, Chile, (2020).

[6] T. P. Barrios, R. Bustinza, G.C. García and M. González, *An a posteriori error analysis of a velocity-pseudostress formulation of the generalized Stokes problem*. Journal of Computational and Applied Mathematics, vol. 357, pp. 349-365, (2019).

[7] T.P. Barrios, R. Bustinza, G. C. García, and E. Hernández, *On stabilized mixed methods for generalized Stokes problem based on the velocity-pseudostress formulation: A priori error estimates.*

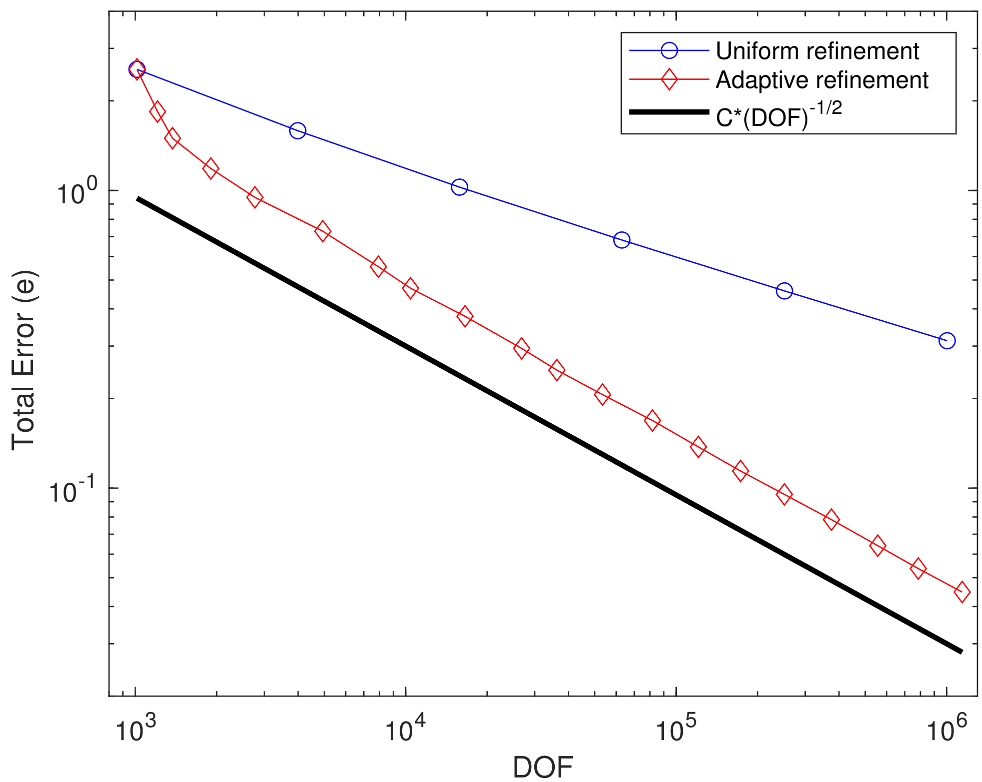

Figure 2: Total error ($\boldsymbol{e}$) vs DOF (N) for uniform and adaptive refinements (Example 2, with $\nu = 1$)

Computer Methods in Applied Mechanics and Engineering, vol. 237-240, pp. 78-87, (2012).

[8] F. Brezzi and M. Fortin. Mixed and hybrid finite element methods. Springer Series in Computational Mathematics 15, Springer-Verlag, New York, 1991.

[9] Z. Cai, B. Lee and P. Wang, *Least-squares methods for incompressible Newtonian fluid flow: Linear stationary problems*. SIAM Journal of Numerical Analysis, vol. 42, pp. 843-859, (2004).

[10] Z. Cai, C. Tong, P.S. Vassilevski and C. Wang. *Mixed finite element methods for incompressible flow: Stationary Stokes equations*. Numerical Methods for Partial Diferential Equations, vol. 26, pp. 957-978, (2010).

[11] C. Carstensen, D. Kim and E.-J. Park, *A priori and a posteriori pseudostress-velocity mixed finite element error analysis for the Stokes problem*, SIAM Journal of Numerical Analysis, vol. 49, 6, pp. 2501-2523, (2011).

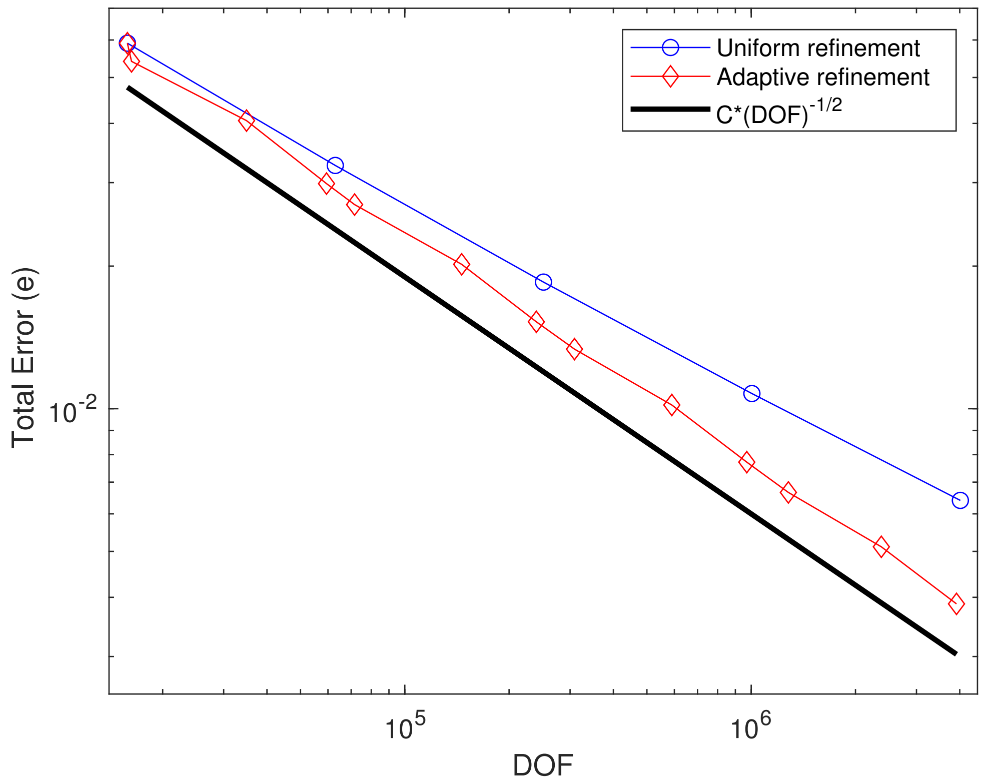

Figure 3: Total error ($\boldsymbol{e}$) vs DOF (N) for uniform and adaptive refinements (Example 3, with $\nu = 1$)

[12] P.G. Ciarlet, The Finite Element Method for Elliptic Problems. North-Holland, 1978.

[13] P. Clément, *Approximation by finite element functions using local regularisation.* RAIRO Modélisation Mathématique et Analyse Numérique, vol. 9, pp. 77-84, (1975).

[14] M. Farhloul and M. Fortin, *A new mixed finite element method for the Stokes and elasticity problems.* SIAM Journal of Numerical Analysis, vol. 30, 4, pp. 971-990, (1993).

[15] M. Farhloul, S. Nicaise and L. Paquet, *A posteriori error estimation for the dual mixed finite element method of the Stokes problem.* Numerical Functional Analysis and Optimization, vol. 27, 7-8, pp. 831-846, (2006).

[16] L. Figueroa, G.N. Gatica and A. Marquez, *Augmented mixed finite element methods for the stationary Stokes equations.* SIAM Journal of Scientific Computing, vol. 31, 2, pp. 1082-1119, (2008).

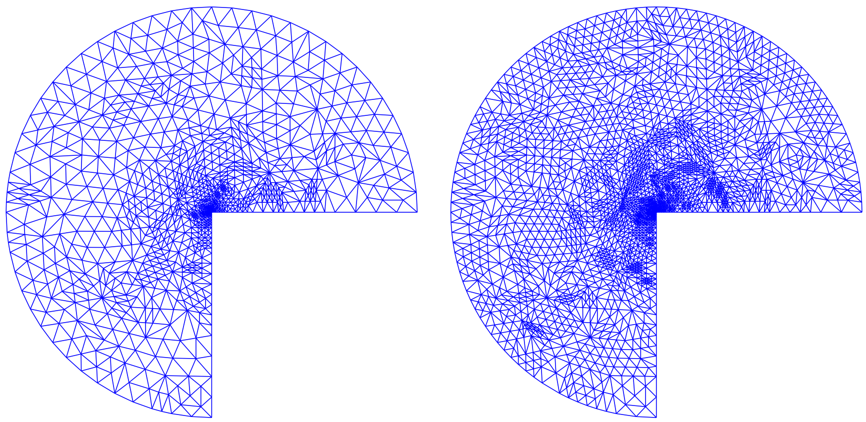

Figure 4: Adaptive refined meshes corresponding to 10417 and 26823 dof (from left to right) (Example 2 with $\nu = 1.0$)

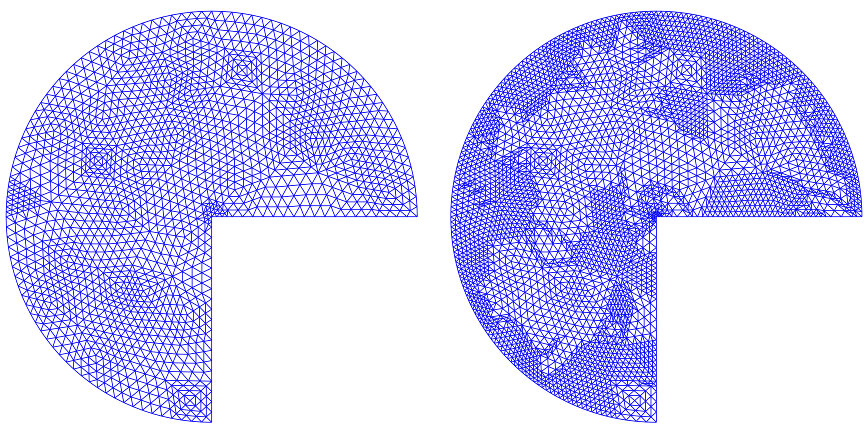

Figure 5: Adaptive refined meshes corresponding to 16259 and 34919 dof (from left to right) (Example 3 with $\nu = 1.0$)

[17] G.N. Gatica, A. Márquez and M.A. Sánchez, *Analysis of a velocity-pressure-pseudostress formulation for the stationary Stokes equations*. Computer Methods in Applied Mechanics and Engineering, vol. 199, pp. 1064-1079, (2010).

[18] G.N. Gatica, A. Márquez and M.A. Sánchez, *A priori and a posteriori error analyses of a velocity-pseudostress formulation for a class of quasi-Newtonian Stokes flows*. Computer Methods in Applied Mechanics and Engineering, vol. 200, pp. 1619-1636, (2011).

[19] V. Girault and P.-A. Raviart, Finite Element Methods for Navier-Stokes Equations. Theory and Algorithms. Springer Verlag, 1986.

[20] R. Hiptmair, *Finite elements in computational electromagnetism.* Acta Numerica, vol. 11, pp. 237-339, (2002).

[21] L.I.G. Kovasznay, *Laminar flow behind a two-dimensional grid*, Mathematical Proceedings of the Cambridge Philosophical Society 44, no. 1, 58-62, (1948).

[22] J.E. Roberts and J.-M. Thomas, *Mixed and Hybrid Methods.* In: Handbook of Numerical Analysis, edited by P.G. Ciarlet and J.L. Lions, vol. II, Finite Element Methods (Part 1), 1991, North-Holland, Amsterdam.

[23] R. Verfürth, *A posteriori error estimation and adaptive mesh-refinement techniques*, Journal of Computational and Applied Mathematics, vol. 50, pp. 67-83, (1994).

[24] R. Verfürth, A Review of a Posteriori Error Estimation and Adaptive Mesh-Refinement Techniques,Wiley-Teubner, Chichester, 1996.

Centro de Investigación en Ingeniería Matemática (CI²MA)

PRE-PUBLICACIONES 2020

2020-16 José Querales, Rodolfo Rodríguez, Pablo Venegas: *Numerical approximation of the displacement formulation of the axisymmetric acoustic vibration problem*

2020-17 Patrick E. Farrell, Luis F. Gatica, Bishnu Lamichhane, Ricardo Oyarzúa, Ricardo Ruiz-Baier: *Mixed Kirchhoff stress - displacement - pressure formulations for incompressible hyperelasticity*

2020-18 David Mora, Iván Velásquez: *Virtual elements for the transmission eigenvalue problem on polytopal meshes*

2020-19 Gabriel N. Gatica, George C. Hsiao, Salim Meddahi: *Further developments on boundary-field equation methods for nonlinear transmission problems*

2020-20 Nicolas Barnafi, Gabriel N. Gatica, Daniel E. Hurtado, Willian Miranda, Ricardo Ruiz-Baier: *New primal and dual-mixed finite element methods for stable image registration with singular regularization*

2020-21 Gonzalo A. Benavides, Sergio Caucao, Gabriel N. Gatica, Alejandro A. Hopper: *A new non-augmented and momentum-conserving fully-mixed finite element method for a coupled flow-transport problem*

2020-22 Raimund Bürger, Elvis Gavilán, Daniel Inzunza, Pep Mulet, Luis M. Villada: *Exploring a convection-diffusion-reaction model of the propagation of forest fires: computation of risk maps for heterogeneous environments*

2020-23 Gabriel N. Gatica, Ricardo Oyarzúa, Ricardo Ruiz-Baier, Yuri D. Sobral: *Banach spaces-based analysis of a fully-mixed finite element method for the steady-state model of fluidized beds*

2020-24 Jessika Camaño, Sergio Caucao, Ricardo Oyarzúa, Segundo Villa-Fuentes: *A posteriori error analysis of a momentum conservative Banach-spaces based mixed-FEM for the Navier-Stokes problem*

2020-25 Raimund Bürger, Julio Careaga, Stefan Diehl: *A method-of-lines formulation for a model of reactive settling in tanks with varying cross-sectional area*

2020-26 Raimund Bürger, Christophe Chalons, Rafael Ordoñez, Luis M. Villada: *A multiclass Lighthill-Whitham-Richards traffic model with a discontinuous velocity function*

2020-27 Tomás Barrios, Edwin Behrens, Rommel Bustinza: *An a posteriori error estimate for a dual mixed method applied to Stokes system with non null source terms*

Para obtener copias de las Pre-Publicaciones, escribir o llamar a: Director, Centro de Investigación en Ingeniería Matemática, Universidad de Concepción, Casilla 160-C, Concepción, Chile, Tel.: 41-2661324, o bien, visitar la página web del centro: http://www.ci2ma.udec.cl




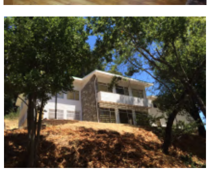

CENTRO DE INVESTIGACIÓN EN
INGENIERÍA MATEMÁTICA (CI^{2}MA)
Universidad de Concepción

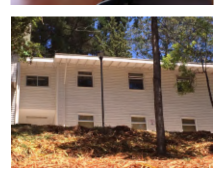
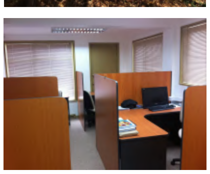

Casilla 160-C, Concepción, Chile
Tel.: 56-41-2661324/2661554/2661316
http://www.ci2ma.udec.cl